



HAL
open science

Use of gas chromatography-mass spectrometry techniques (GC-MS, GC-MS/MS and GC-QTOF) for the characterization of lipid photooxidation and autoxidation products in senescent autotrophic organisms

Jean-Francois Rontani

► **To cite this version:**

Jean-Francois Rontani. Use of gas chromatography-mass spectrometry techniques (GC-MS, GC-MS/MS and GC-QTOF) for the characterization of lipid photooxidation and autoxidation products in senescent autotrophic organisms. *Molecules*, 2022, 27 (5), pp.1629. 10.3390/molecules27051629 . hal-03605143

HAL Id: hal-03605143

<https://hal.science/hal-03605143>

Submitted on 10 Mar 2022

HAL is a multi-disciplinary open access archive for the deposit and dissemination of scientific research documents, whether they are published or not. The documents may come from teaching and research institutions in France or abroad, or from public or private research centers.

L'archive ouverte pluridisciplinaire **HAL**, est destinée au dépôt et à la diffusion de documents scientifiques de niveau recherche, publiés ou non, émanant des établissements d'enseignement et de recherche français ou étrangers, des laboratoires publics ou privés.

1 Review

2 Use of gas chromatography-mass spectrometry techniques (GC- 3 MS, GC-MS/MS and GC-QTOF) for the characterization of li- 4 pid photooxidation and autoxidation products in **senescent** au- 5 totrophic organisms

6 Jean-François Rontani ^{1*}7 ¹ Aix Marseille Univ, Université de Toulon, CNRS, IRD, MIO UM 110, Marseille, France, 13288, Marseille,
8 France; jean-francois.rontani@mio.osupytheas.fr

9 * Correspondence: jean-francois.rontani@mio.osupytheas.fr; Tel.: 33 (0)4 86 09 06 02

Abstract: This paper reviews applications of gas chromatography-mass spectrometry techniques for the characterization of lipid photooxidation and autoxidation products in senescent phototrophic organisms. Particular attention is given to: (i) the selection of oxidation products that are sufficiently stable and specific to each lipid class and degradation route, (ii) the description of electron ionization mass fragmentation of trimethylsilyl derivatives of these compounds and (iii) the use of specific fragment ions for monitoring the oxidation of the main unsaturated lipid components of phototrophs. The techniques best geared for this task were gas chromatography-quadrupole-time of flight to monitor fragment ions with very high resolution and accuracy, and gas chromatography-tandem mass spectrometry to monitor very selective transitions in multiple reaction monitoring mode. The extent of the degradation processes can only be estimated if the oxidation products are unaffected by fast secondary oxidation reactions, as it is notably the case of Δ^5 -sterols, monounsaturated fatty acids, chlorophyll phytyl side-chain, and di- and triterpenoids. In contrast, the primary degradation products of highly branched isoprenoid alkenes possessing more than one trisubstituted double bond, alkenones, carotenoids and polyunsaturated fatty acids, appear to be too unstable with respect to secondary oxidation or other reactions to serve for quantification in **senescent** phototrophs.

Citation: Rontani J.-F. Use of gas chromatography-mass spectrometry techniques (GC-MS, GC-MS/MS and GC-QTOF) for the characterization of lipid photooxidation and autoxidation products in autotrophic organisms. *Molecules* **2022**, *27*, x. <https://doi.org/10.3390/xxxxx>

Academic Editor: Firstname Lastname

Received: date

Accepted: date

Published: date

Publisher's Note: MDPI stays neutral with regard to jurisdictional claims in published maps and institutional affiliations.



Copyright: © 2022 by the authors. Submitted for possible open access

Keywords: Senescent phototrophs; Unsaturated lipids; Photooxidation; Autoxidation; Gas chromatography-mass spectrometry; Specific tracers; TMS derivatives; EI fragmentation.

1. Introduction

Phototrophic organisms (mainly green plants, algae, cyanobacteria and some protists) carry out photosynthesis *i.e.* conversion of sunlight energy, carbon dioxide and water into organic materials. Due to the generation of highly reactive oxygen species (ROS) during photosynthetic electron transport, these organisms are particularly sensitive to oxidative damages [1]. Lipids (hydrocarbons, pigments, terpenoids, free fatty acids, acylglycerides, phospholipids, galactolipids, cutins, suberins and waxes [2]) are important components of phototrophic organisms, accounting for 16-26% of organic content in phytoplankton [3] and up to 45% in the green alga *Botryococcus Braunii* [4]. The relative stability and specificity of lipids makes them popular tracers of the origin of organic matter in environmental samples [5-7]. Their abiotic oxidation products can be also very useful for estimating present or past photooxidative and autoxidative alterations in specific phototrophic organisms [8,9].

The most common chromatographic methods for lipid analysis are gas chromatography (GC), and high-performance liquid chromatography (HPLC) coupled with mass

publication under the terms and
conditions of the Creative Commons
Attribution (CC BY) license
(<https://creativecommons.org/licenses/by/4.0/>).

spectrometers (MS). GC-based analytical procedures requires analytes that are volatile and thermally stable. In practice, this means that GC-based analysis of the oxidation products of mixtures of complex and simple lipids with such techniques demands a chemical pre-treatment of the samples, including: (i) NaBH₄ reduction of thermally-labile hydroperoxides to the corresponding alcohols [10], (ii) alkaline hydrolysis of complex lipids into their constituent fatty acids, plus glycerol, phosphate, sterol or sugar groups [5], and then (iii) conversion of polar compounds to volatile derivatives (derivatization). Despite this added time-consuming pre-treatment (which is not necessary with HPLC-MS analyses), GC-MS techniques involving electron ionization (EI) and chemical ionization (CI) are widely employed for the characterization of lipid oxidation products [11-13]. Indeed, EI provides more structural information than the soft ionization techniques such as electron spray ionization (ESI) or atmospheric pressure chemical ionization (APCI) employed in HPLC-MS analyses, notably as it enables easy determination of the position of functional groups of lipid oxidation products [14]. However, the relatively soft ESI and APCI ionization modes used during HPLC-MS analyses allow structural characterization of thermally-labile compounds (e.g. hydroperoxides) [15]. Moreover, the possibility to work in reverse-phase liquid chromatography also allows the analysis of compounds too heavy or polar to be amenable by GC (e.g. triacylglycerides) [15,16]. Note that other powerful non-chromatographic techniques such as matrix-assisted laser desorption/ionization mass spectrometry (MALDI-MS) [17,18], ion-mobility mass spectrometry (IM-MS) [19,20], and nuclear magnetic resonance (NMR) [21] also appeared to be very useful for the characterization of lipid oxidation products.

In this review, particular attention is given to the use of gas chromatography-tandem mass spectrometry (GC-MS/MS) and gas chromatography-quadrupole-time of flight (GC-QTOF) techniques for the characterization of trimethylsilyl (TMS) derivatives of lipid oxidation products in senescent phototrophic organisms. GC-MS/MS can perform analyses in multiple reaction monitoring (MRM) mode based on specific collision-induced fragmentations of precursor ions, which substantially increase signal-to-noise ratios and method sensitivity [22]. GC-QTOF offers high mass resolution and accuracy, and can use narrow mass intervals reducing interferences and background noise, making it particularly suitable for identifying unknown lipid oxidation products in complex natural extracts.

Trimethylsilylation is the method most commonly employed for derivatization of lipids in GC-MS analyses [23,24]. TMS derivatives are produced by replacing the active hydrogen atom of alcohols, acids, amines and thiols by a trimethylsilyl group. These derivatives are highly volatile, thermally stable and present outstanding gas chromatographic characteristics. EI mass spectra of TMS derivatives generally exhibit a significant [M -15]⁺ ion formed by loss of a silicon-bonded methyl group, which is especially useful for determining molecular mass. Fragmentations of these derivatives are also hugely informative for structural elucidations [25,26].

2. Abiotic oxidation of lipid components of autotrophic organisms

2.1. Type II photosensitized oxidation

Due to the presence of chlorophyll, which is a very efficient photosensitizer [27,28], visible light-induced photosensitized processes act intensively during the senescence of autotrophic organisms. In healthy cells, the excited singlet state of chlorophyll (¹Chl) formed after absorption of a quantum of light energy, leads predominantly to the characteristic fast photosynthesis reactions [27]. However, a small proportion of ¹Chl undergoes intersystem crossing (ISC) to form the longer live triplet state (³Chl) [28], which is not only itself potentially damaging in type I reactions [28] but can also generate ROS and, in particular, singlet oxygen (¹O₂) by reacting with ground state oxygen (³O₂) (type

II processes). As a defense against oxidative damage, there are many antioxidant compounds (e.g. carotenoids and vitamin E) and enzymes (e.g. superoxide dismutase and catalase) that operate in chloroplasts [27,29].

As fast photosynthesis reactions are clearly not operative in senescent phototrophic organisms, potentially damaging ^3Chl and $^1\text{O}_2$ [30] are produced at an accelerated rate exceeding the quenching capacity of the photoprotective system and thus damage the membranes (photodynamic effect [31]). $^1\text{O}_2$ readily oxidizes cellular components of senescent autotrophic organisms such as unsaturated lipids (including Δ^5 -sterols, unsaturated fatty acids, chlorophyll phytyl side-chain, carotenoids and alkenes), proteins, and nucleic acids [32]. The rate of reaction of $^1\text{O}_2$ with olefins is controlled by the degree of substitution and the configuration (*cis*- or *trans*-) of the double bond [33], with highly-substituted and *cis*- double bonds being the more reactive. Type II photosensitized oxidation of unsaturated lipids affords allylic hydroperoxides (for reviews see [8,9]).

2.2. Free radical oxidation (autoxidation)

Due to spin restriction [34], the unpaired electrons of ground-state triplet molecular oxygen $^3\text{O}_2$ can only interact with unpaired electrons of organic radicals, which drive autoxidation reactions. Autoxidation involves free-radical-mediated oxidation chain reactions, which can be divided into three steps: chain initiation, propagation, and termination [35]. Initiation of autoxidation requires initiators that are able to produce radicals by removing an electron to the substrate molecule or breaking a covalent bond. The most common initiators are heat, light, redox-active metal ions undergoing one-electron transfer (e.g. Fe^{2+} , Co^{2+} , Fe^{3+} , Cu^{2+} , Mn^{2+} , Zn^{2+} , Mg^{2+} , V^{2+}), and certain enzymes (lipoxygenases). The propagation step involves a succession of reactions in which each radical produced in one reaction is consumed in the next [36]. It generally proceeds via: (i) hydrogen atom abstraction from tertiary, allylic or α to oxygen positions, and (ii) addition of peroxy radicals to double bonds. Termination results from reactions of radicals affording non-radical products. In senescent phototrophic cells, initiation of autoxidation processes is generally attributed to the cleavage (induced by heat, light, metals or enzymes) of hydroperoxides resulting from type II photosensitized oxidation of cellular components to hydroxyl, peroxy and alkoxy radicals [37,38].

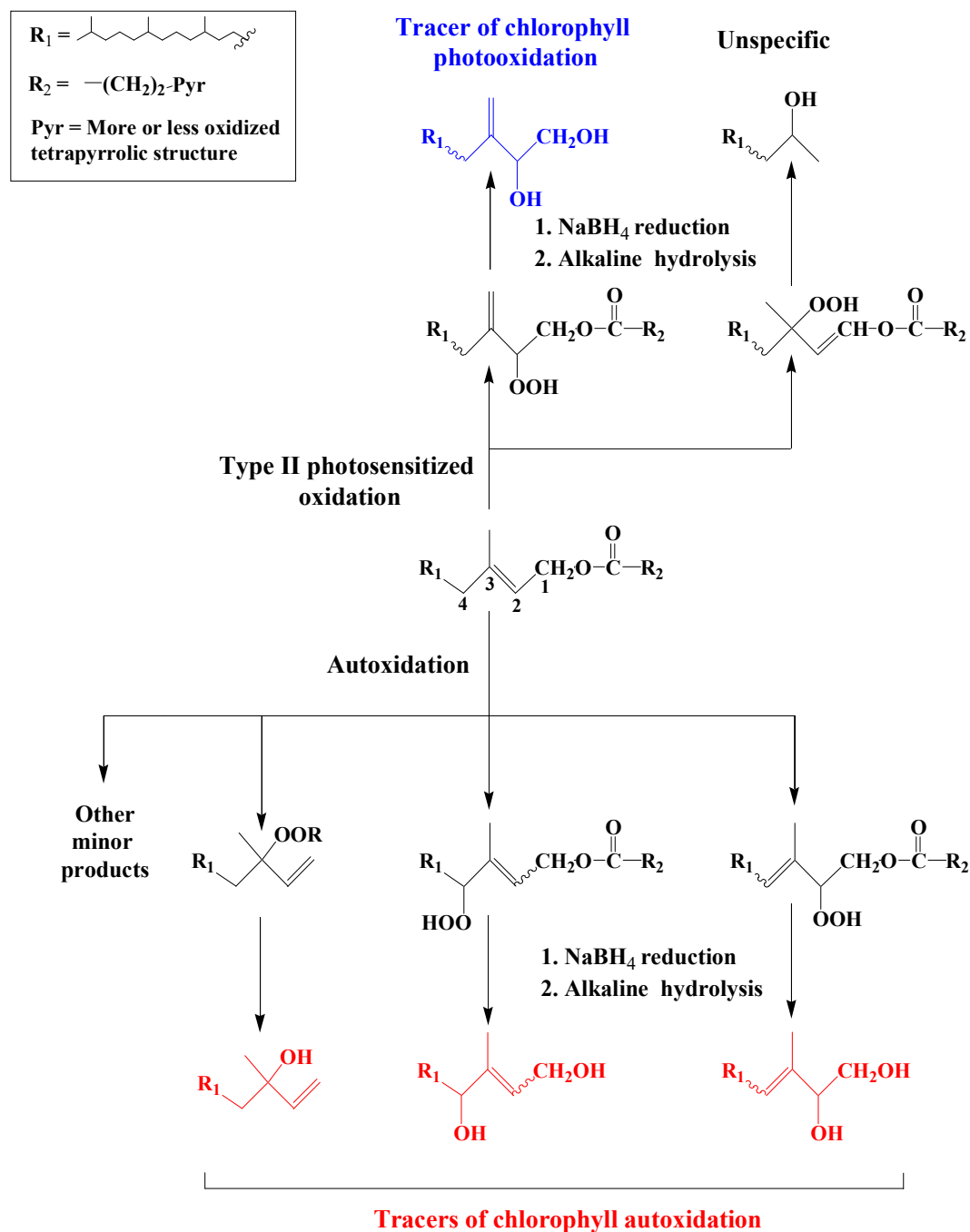
3. Characterization of the oxidation products of lipids

This chapter briefly describes the mechanisms of photooxidation and autoxidation of the main unsaturated lipids of phototrophic organisms. A focus is given to the selection of **oxidation products sufficiently** stable and specific **to act as** tracers of these processes **under environmental conditions**, as well as to the mechanisms of fragmentation of TMS derivatives of these compounds during electron ionization. Some application examples of these tracers are also shown. Note that accurate masses of the different fragment ions formed are given, which makes them amenable to use in GC-QTOF analyses, while the corresponding unit masses can still be used in GC-MS/MS or classical GC-MS analyses.

3.1. Chlorophyll phytyl side-chain

Attack of $^1\text{O}_2$ on the tri-substituted double bond of the chlorophyll phytyl side-chain affords two allylic hydroperoxides, which may be recovered in the form of 6,10,14-trimethylpentadecan-2-ol and 3-methylidene-7,11,15-trimethylhexadecan-1,2-diol (phytyldiol) after NaBH_4 reduction and alkaline hydrolysis [39] (Scheme 1). The stable and highly specific phytyldiol was proposed as biogeochemical marker of chlorophyll photodegradation in the natural environment [40]. In contrast, free radical oxidation (autoxidation) of chlorophyll phytyl side-chain and subsequent reduction and hydrolysis

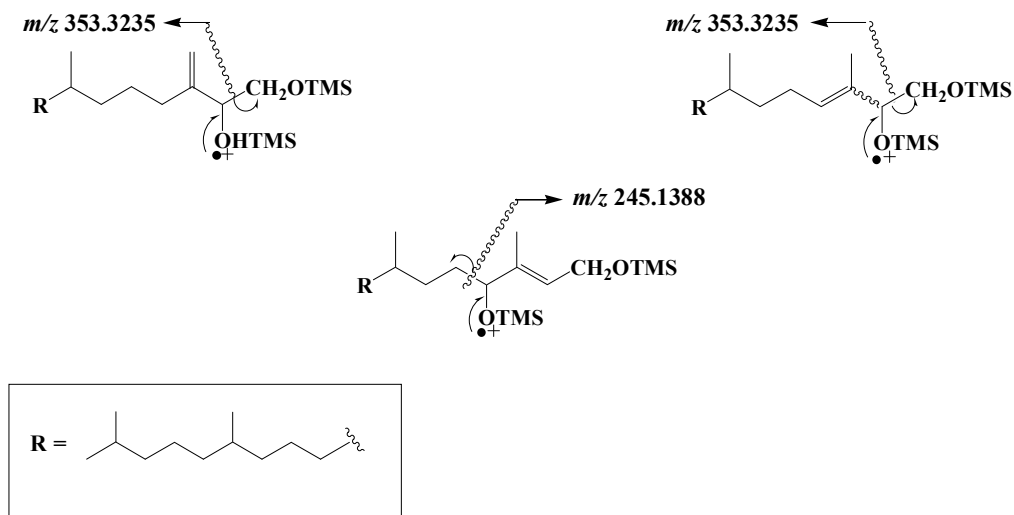
gives 3,7,11,15-tetramethylhexadec-3-en(*Z/E*)-1,2-diols, 3,7,11,15-tetramethyl-hexadec-2-en(*Z/E*)-1,4-diols and 3,7,11,15-tetramethyl-hexadec-1-en-3-ol (isophytol) [41,42] (Scheme 1). These compounds have been proposed as specific tracers of chlorophyll phytyl side-chain autoxidation in environmental samples [41,42].



Scheme 1. Photooxidation and autoxidation of chlorophyll phytyl side-chain.

TOF mass spectra of the TMS derivatives of phytyldiol and 3,7,11,15-tetramethylhexadec-3-en(*Z/E*)-1,2-diols show intense and specific fragment ions at m/z 353.3235 resulting from classical α -cleavage between the carbon atoms 1 and 2 bearing

the two TMS ether groups [31], while the spectra of TMS derivatives of 3,7,11,15-tetramethyl-hexadec-2-en(*Z/E*)-1,4-diols are dominated by a fragment ion at m/z 245.1388 corresponding to α -cleavage between carbon atoms 4 and 5 (Scheme 2).



Scheme 2. Main EI mass fragmentations of TMS derivatives of phytyldiol, 3,7,11,15-tetramethylhexadec-3-en(*Z/E*)-1,2-diols and 3,7,11,15-tetramethyl-hexadec-2-en(*Z/E*)-1,4-diols.

Note that the loss of a methyl radical by the molecular ion of TMS derivatives of phytol and isophytol also affords a fragment ion at m/z 353.3235. Monitoring ions at m/z 353.3235 and 245.1388 thus allows simultaneous characterization and quantification of phytol and its main photooxidation and autoxidation products in natural samples (see example given in Fig. 1).

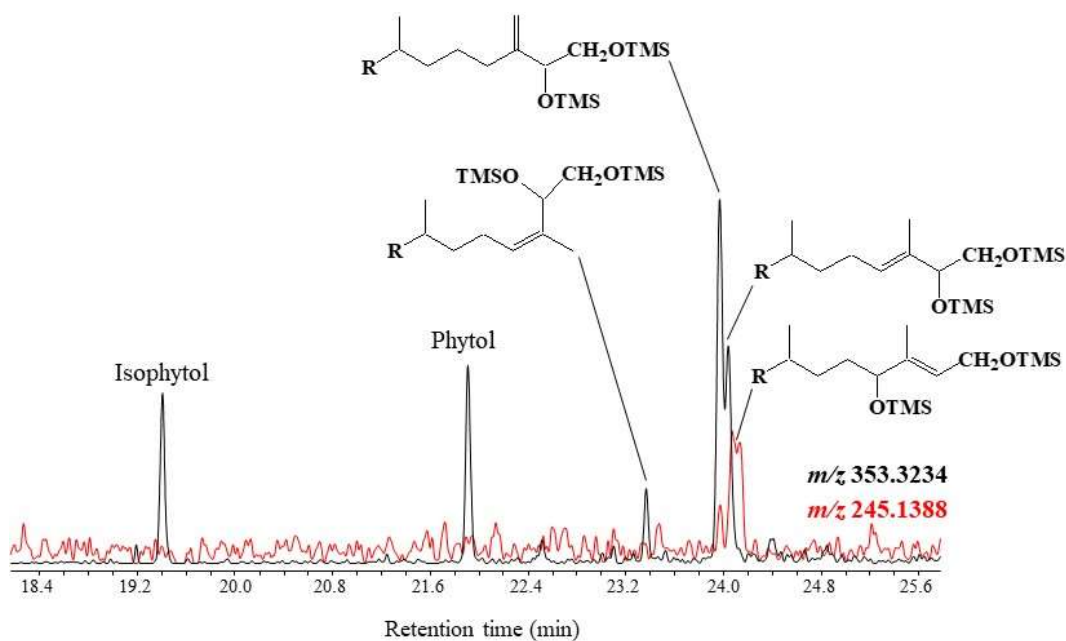
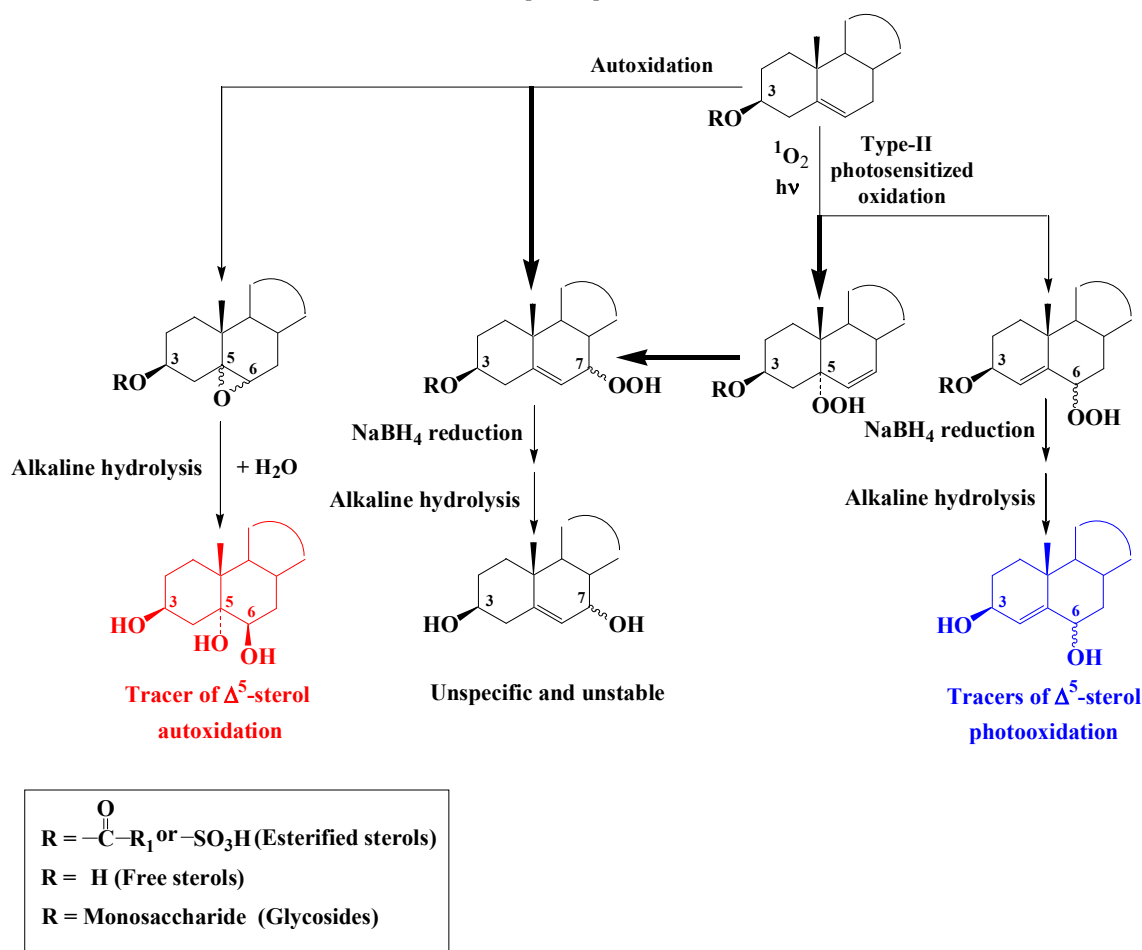


Figure 1. Partial TOF ion chromatograms (m/z 353.3235 and 245.1388) showing the presence of TMS derivatives of phytol and its main photooxidation and autoxidation products in senescent cells of the diatom *Thalassiosira* sp.

3.23. Δ^5 -sterols

Reaction of $^1\text{O}_2$ with the double bond of Δ^5 -sterols mainly affords a Δ^6 -5 α -hydroperoxide and to a lesser extent Δ^4 -6 α/β -hydroperoxides [43,44] (Scheme 3). Under environmental conditions Δ^6 -5 α -hydroperoxide undergoes fast allylic rearrangement to unstable and unspecific 7 α/β -hydroperoxides (Scheme 3). Δ^4 -Stero-3 β ,6 α/β -diols resulting from NaBH_4 -reduction and alkaline hydrolysis of Δ^4 -6 α/β -hydroperoxides were thus proposed as specific tracers of type II photosensitized oxidation of the corresponding Δ^5 -sterols [45,46].

Autoxidation of Δ^5 -sterols mainly affords unstable and unspecific 7 α/β -hydroperoxides after hydrogen atom abstraction at the allylic carbon atom 7 [47] (Scheme 3). Smaller proportions of isomeric 5 α ,6 α - and 5 β ,6 β -epoxysterols are also produced after addition of peroxy radical to the double bond [48] (Scheme 3). Stable and specific 3 β ,5 α ,6 β -trihydroxysterols resulting from the hydrolysis of these epoxides during alkaline hydrolysis and in environmental conditions were proposed as specific tracers of the autoxidation of Δ^5 -sterols [45,46].

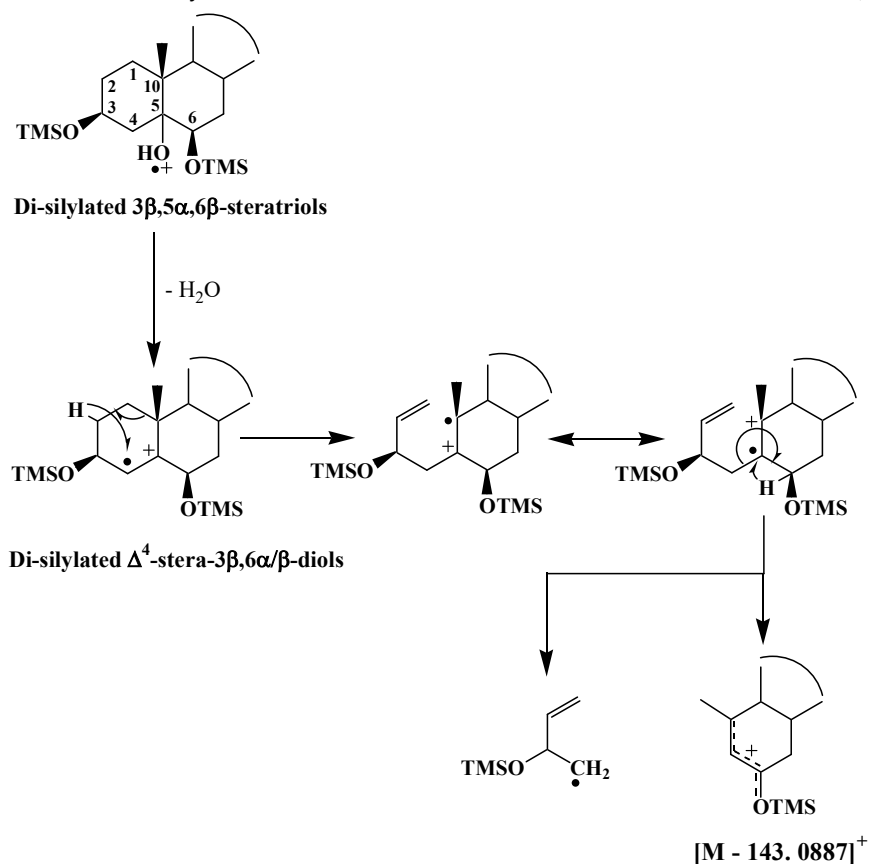


Scheme 3. Photooxidation and autoxidation of Δ^5 -sterols.

TOF mass spectra of Δ^4 -stero-3 β ,6 α/β -diol TMS derivative exhibit an intense and interesting fragment ions at $[\text{M} - 143.0887]^+$ resulting from double bond ionization and subsequent hydrogen migrations and cleavages of the C_1-C_{10} and C_4-C_5 bonds [49] (Scheme 4). Due to steric hindrance, the classical silylation reagents only silylate 3 β ,5 α ,6 β -trihydroxysterols to their 3 and 6 positions [50], and during ionization their

204
205

TMS derivatives very easily lose a neutral molecule of water and thus exhibit mass spectra that are very similar to those of Δ^4 -stera-3 β ,6 β -diol TMS derivatives (Scheme 4).

206
207
208
209
210
211
212

Scheme 4. Proposed formation pathways of the fragment ion $[M - 143.0887]^+$ in TOF mass spectra of Δ^4 -stera-3 β ,6 β -diol and 3 β ,5 α ,6 β -trihydroxysterol TMS derivatives.

Table 1. Accurate masses of the $[M - 143.0887]^+$ fragment ion of TMS derivatives of Δ^4 -stera-3 β ,6 β -diols arising from the more common Δ^5 -sterols.

Δ^5 -sterols	$[M - 143.0887]^+$
24-Nor-cholesta-5,22-dien-3 β ,6 α/β -diols	387.3084
24-Nor-cholest-5-en-3 β ,6 α/β -diols	389.3240
Cholesta-5,22-dien-3 β ,6 α/β -diols	401.3240
Cholesta-5,24-dien-3 β ,6 α/β -diols	401.3240
Cholest-5-en-3 β ,6 α/β -diols	403.3396
24-Methylcholest-5-en-3 β ,6 α/β -diols	417.3562
24-Methylcholesta-5,22-dien-3 β ,6 α/β -diols	415.3396
24-Methylcholesta-5,24/28-dien-3 β ,6 α/β -diols	415.3396
24-Ethylcholest-5-en-3 β ,6 α/β -diols	431.3710
24-Ethylcholesta-5,22-dien-3 β ,6 α/β -diols	429.3552

213
214
215
216
217
218
219

Specific fragment ions $[M - 143.0887]^+$, for which Table 1 gives accurate masses for the Δ^4 -stera-3 β ,6 β -diols of the more common sterols, thus emerged as very useful for the monitoring of Δ^5 -sterol photooxidation and autoxidation in phototrophic organisms. An example of their application is given in Fig. 2.

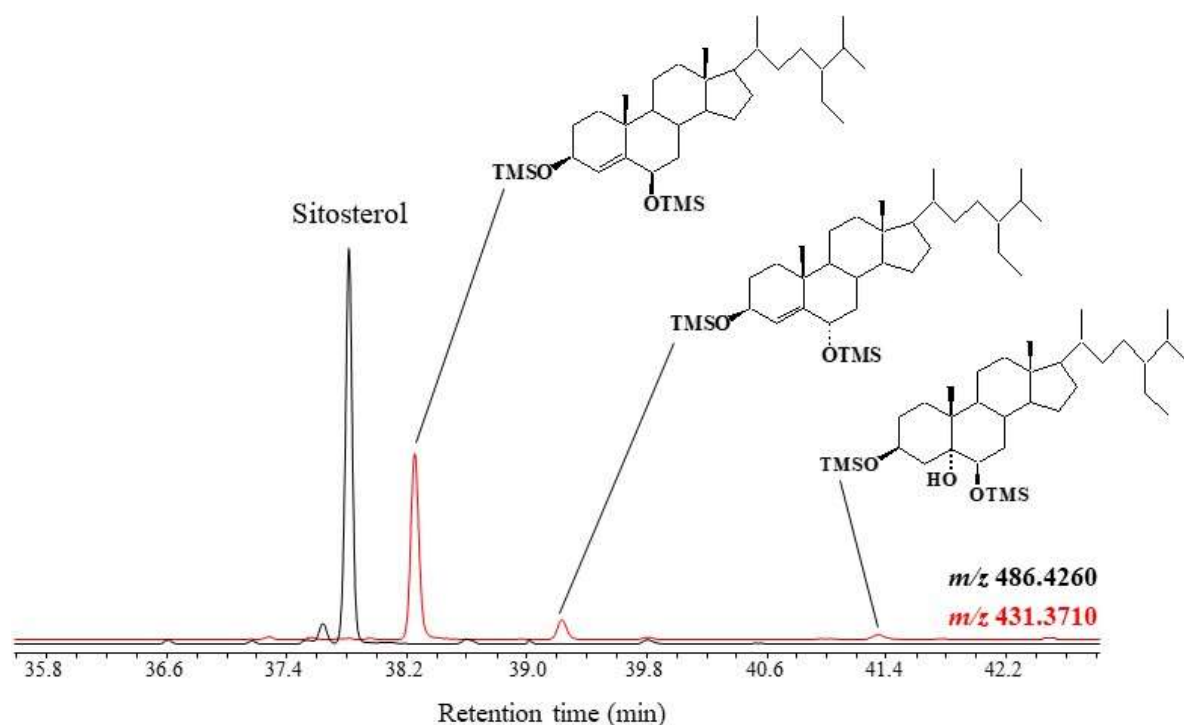
220
221
222
223
224
225
226
227

Figure 2. Partial TOF ion chromatogram (m/z 431.3710 and 486.4260) showing the presence of TMS derivatives of 24-ethylcholest-5-en-3 β -ol (sitosterol) ($[M]^+ = 486.4260$) and its photo- ($[M - 143.0887]^+ = 431.3710$) and autoxidation ($[M - H_2O - 143.0887]^+ = 431.3710$) products in senescent leaves of *Smilax aspera*.

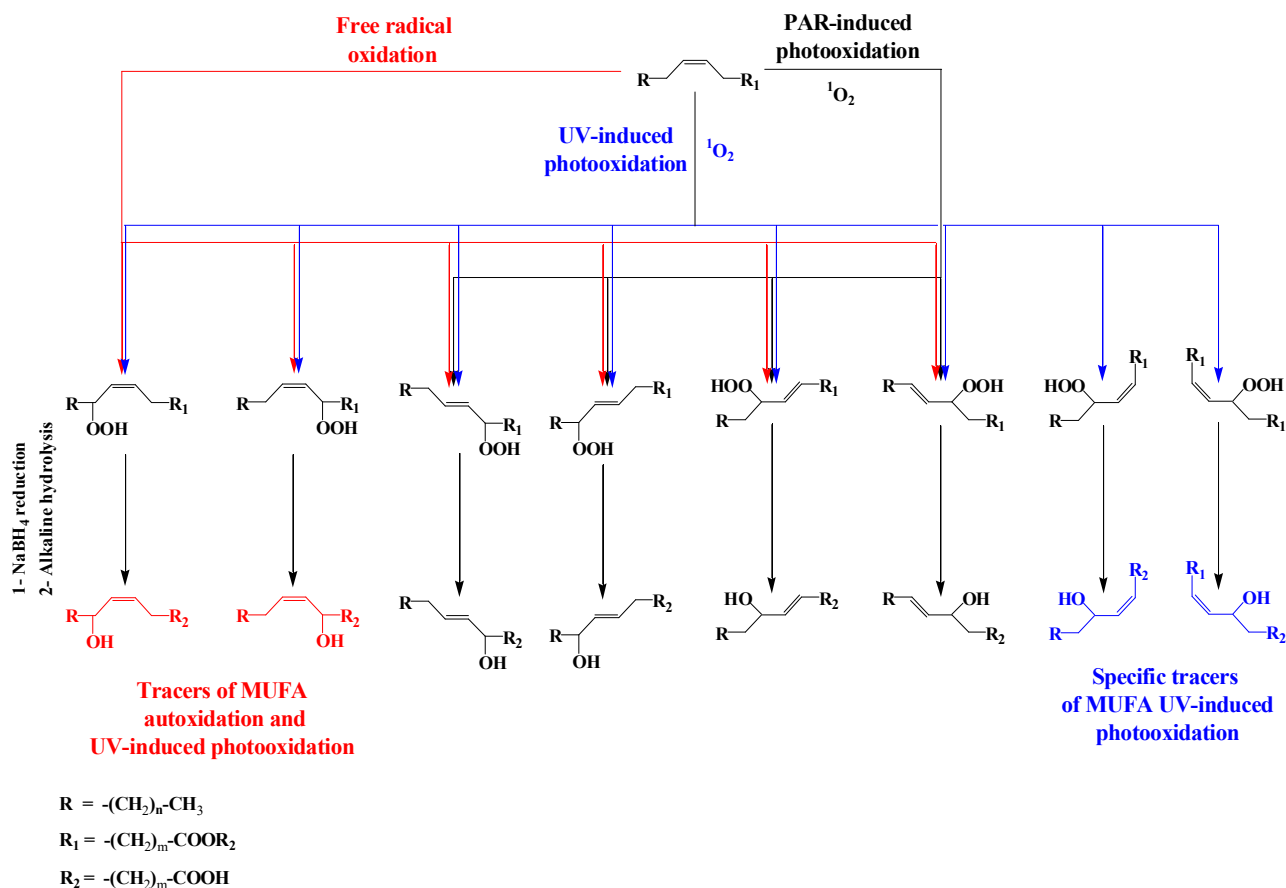
3.34. Unsaturated fatty acids

228
229
230
231
232
233
234
235
236
237
238
239
240
241
242
243

Type II photosensitized oxidation and autoxidation rates of unsaturated fatty acids logically increase with their number of double bonds [51,52]. Unfortunately, oxidation products of the more reactive polyunsaturated fatty acids (PUFAs) are not sufficiently stable under environmental conditions to be used as tracers of these degradation processes *in situ*. Note that isoprostanooids (cyclopentane-containing oxylipins) resulting from autoxidation of C₁₈, C₂₀ and C₂₂ PUFAs are often used as biomarkers for *in vivo* oxidative stress in animals and plants [53]. These compounds could be detected in higher plants and algae by using GC-MS in negative-ion chemical ionization (NICI) mode [53,54]. However, in the literature there are no reports of such compounds in environmental samples.

In contrast, oxidation products of monounsaturated fatty acids (MUFAs) are sufficiently stable for use as tracers of type-II photosensitized oxidation and autoxidation processes *in situ* [10]. During type II photosensitized oxidation of MUFAs, attack by 1O_2 of the two ethylenic carbon atoms of the double bond leads to the formation of two *trans*-allylic hydroperoxides [52,55], which subsequently undergo stereoselective radical allylic rearrangement to afford two other isomers with a *trans*-

double bond [56] (Scheme 5). Note that if type II photosensitized oxidation of MUFAs involves UV radiation, then four corresponding *cis*- allylic hydroperoxides also get produced [57] (Scheme 5). In contrast, free radical oxidation of these compounds affords only two *cis*- allylic hydroperoxides (corresponding to the oxidation of the two allylic positions of MUFAs) in addition to the four *trans*- isomeric hydroperoxides [56] (Scheme 5). Consequently, in *senescent* autotrophic organisms a dominance of these two *cis*- isomers (among the four *cis*- isomers) points to the involvement of autoxidation processes, while a dominance of all four *cis*- isomers points to UV-induced photodegradation.

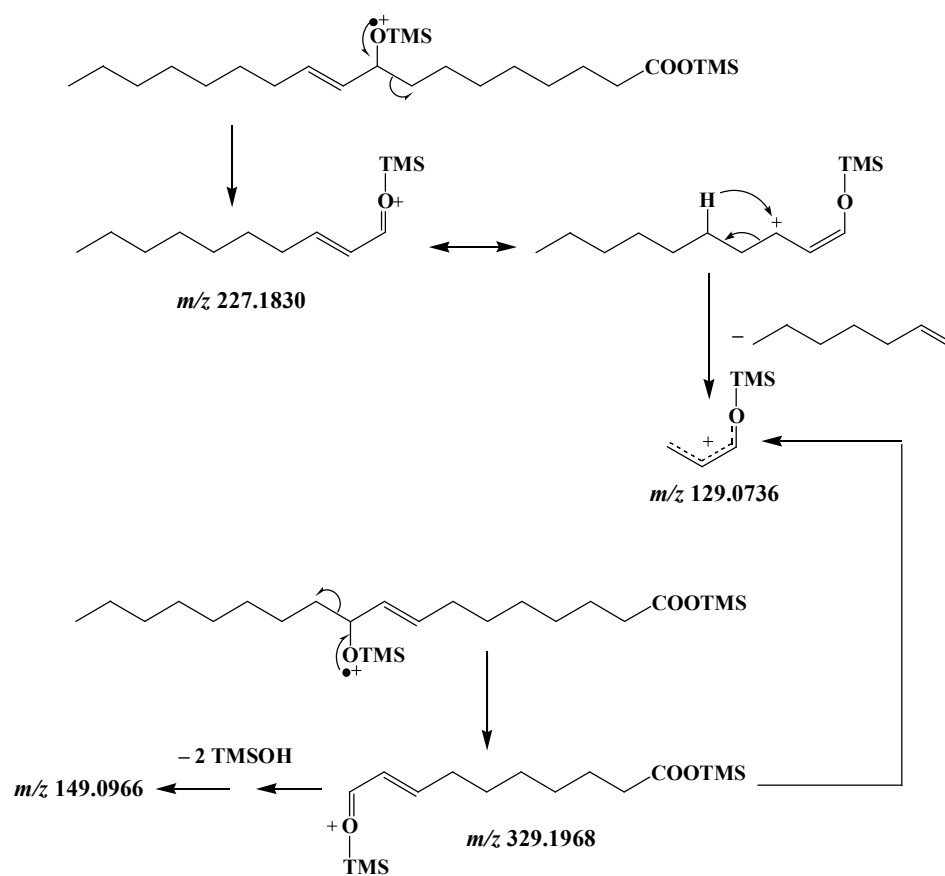


Scheme 5. Type II photosensitized oxidation (induced by PAR and UV radiations) and autoxidation of MUFAs.

Under EI TMS derivatives of isomeric allylic hydroxyacids resulting from photooxidation and autoxidation of MUFAs and subsequent $NaBH_4$ reduction undergo α -cleavage at their TMS ether group. Cleavage acts on the saturated side of the molecule (as the vinylic position of the double bond hinders cleavage on the other side) and affords stable and specific fragment ions (Scheme 6) that are dependent on the carbon atom number and double-bond position of the MUFA considered [11,15]. The fragment ions resulting from α -cleavage of silylated oxidation products of the more common MUFAs are listed in Table 2.

269
270
271
272**Table 2.** Accurate masses of the main fragment ions produced during EI fragmentation of silylated allylic hydroxyacids resulting from NaBH₄-reduction of photo- and autoxidation products of some common MUFAs.

MUFAs	(OH-position) <i>m/z</i>	(OH-position) <i>m/z</i>	(OH-position) <i>m/z</i>	(OH-position) <i>m/z</i>
C _{16:1} 9	(9-) 199.1518 ^a	(8-) 213.1675 ^a	(10-) 329.1968 ^b	(11-) 343.2125 ^b
C _{16:1} 11	(11-) 171.1206	(10-) 185.1363	(12-) 357.2280	(13-) 371.2437
C _{18:1} 9	(9-) 227.1830	(8-) 241.1987	(10-) 329.1968	(11-) 343.2125
C _{18:1} 11	(11-) 199.1518	(10-) 213.1675	(12-) 357.2280	(13-) 371.2437
C _{20:1} 9	(9-) 255.2139	(8-) 269.2295	(10-) 329.1968	(11-) 343.2125
C _{20:1} 11	(11-) 227.1830	(10-) 241.1987	(12-) 357.2280	(13-) 371.2437
C _{22:1} 9	(9-) 283.2451	(8-) 297.2607	(10-) 329.1968	(11-) 343.2125
C _{22:1} 11	(11-) 255.2139	(10-) 269.2295	(12-) 357.2280	(13-) 371.2437

273
274
275^a Fragments containing the terminal methyl group.^b Fragments containing the trimethylsilyl ester group.276
277
278
279**Scheme 6.** Examples of EI fragmentations of TMS derivatives of MUFA oxidation products.

280
281
282
283

GC-QTOF allows a clean characterization and quantification of TMS derivatives of MUFA oxidation products in autotrophic organisms and environmental samples. Fig. 3 gives some examples of the technique application showing typical profiles of visible light-induced, (visible + UV) light-induced and autoxidative degradation products.

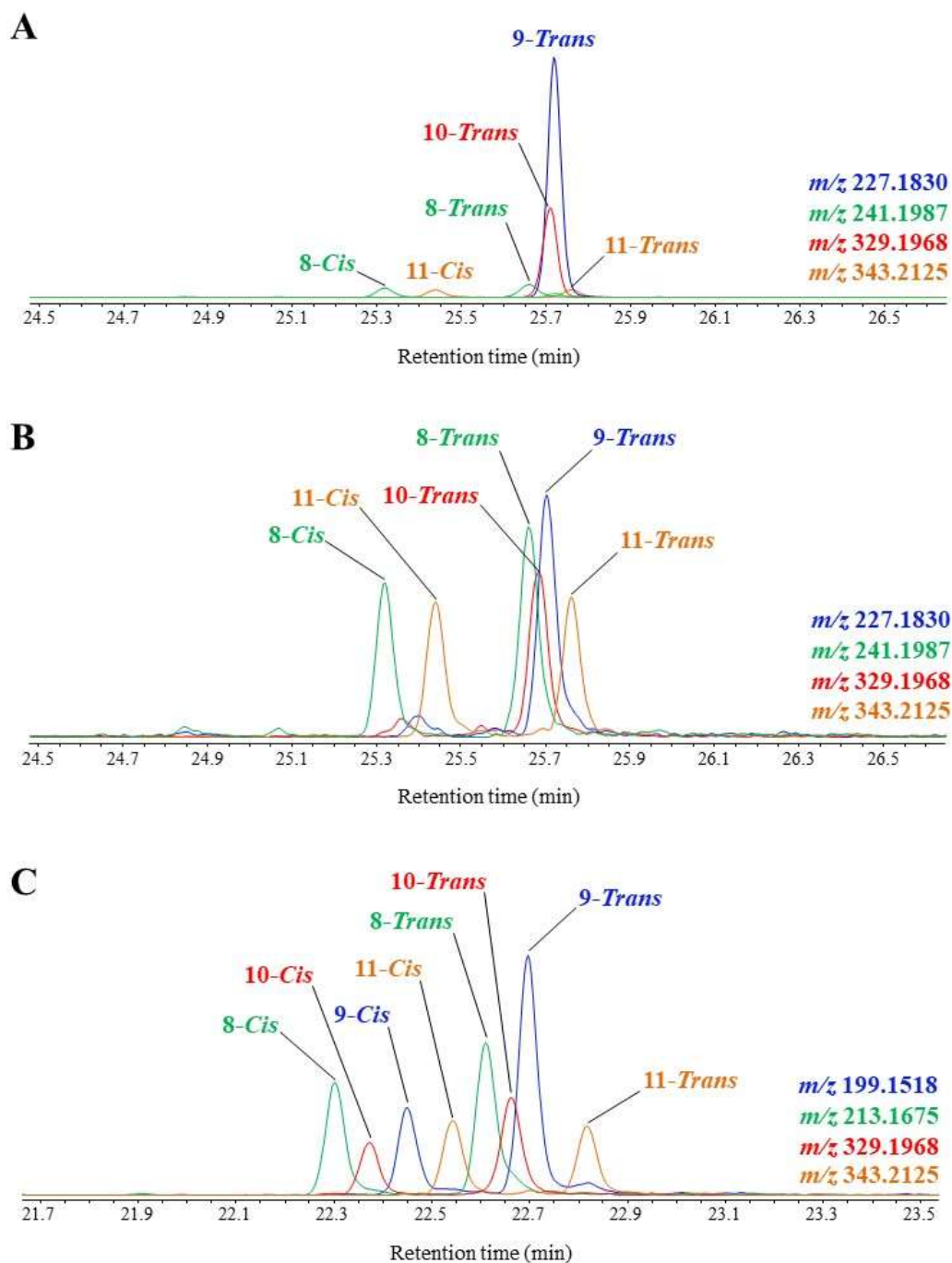
284
285
286
287
288
289

Figure 3. Partial TOF ion chromatograms showing TMS derivatives of MUFA oxidation products in senescent cells of the haptophyte *Emiliania huxleyi* irradiated by visible light (A), and after aging (B), and of the diatom *Thalassiosira* sp. irradiated by (visible + UV) light (C).

290
291
292

MRM analyses of TMS derivatives of MUFA oxidation products involve intense and selective transitions from the ions resulting from α -cleavage (precursor ions) to the fragment ion at m/z 129 (product ion) (Scheme 6). Note that this transition is more

efficient with precursor ions containing the terminal methyl group than with precursor ions containing the TMS ester group, which can easily lose neutral TMSOH molecules (Scheme 6, Fig. 4). Fig. 5 gives an example of how MRM analyses can be applied.

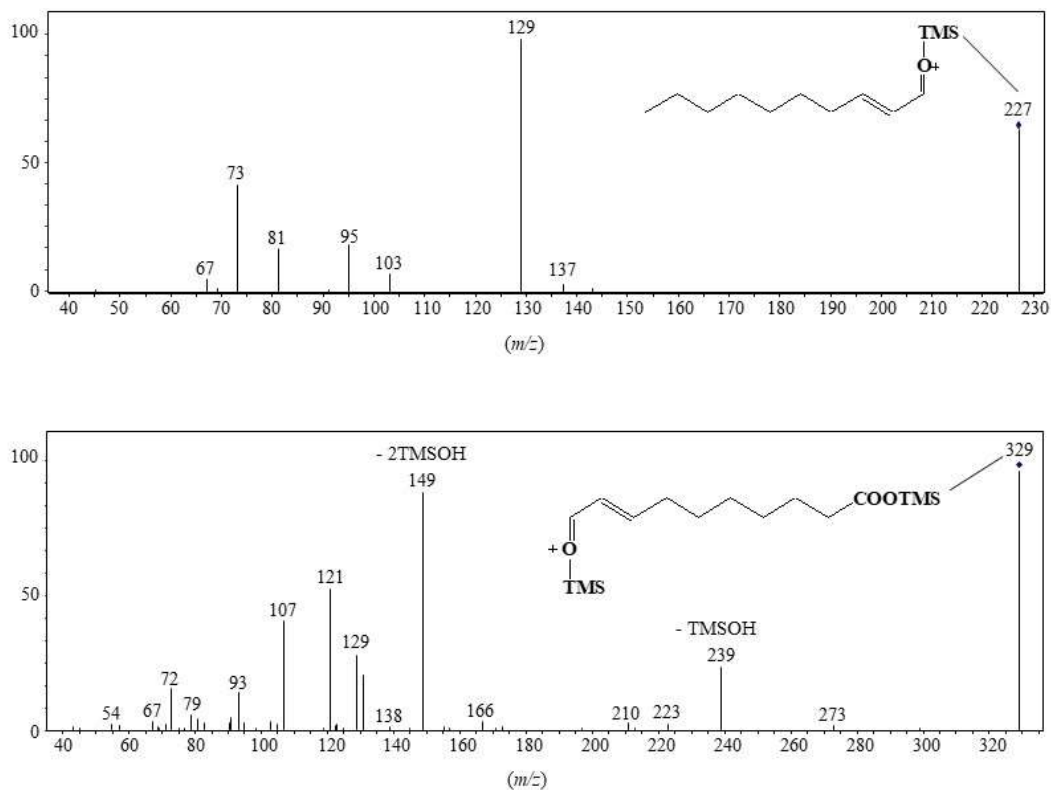


Figure 4. Collision-induced dissociation (CID) (5 eV) of fragment ions at m/z 227 and 329.

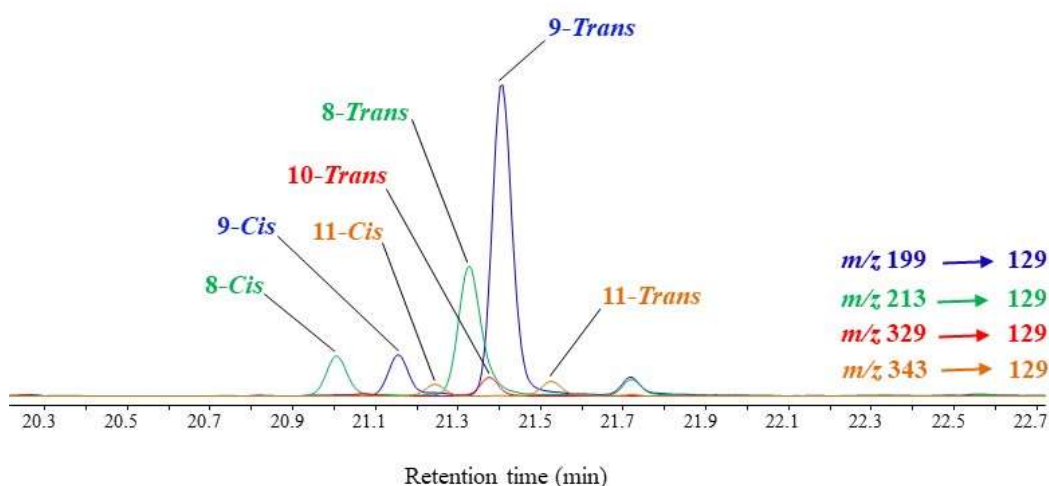


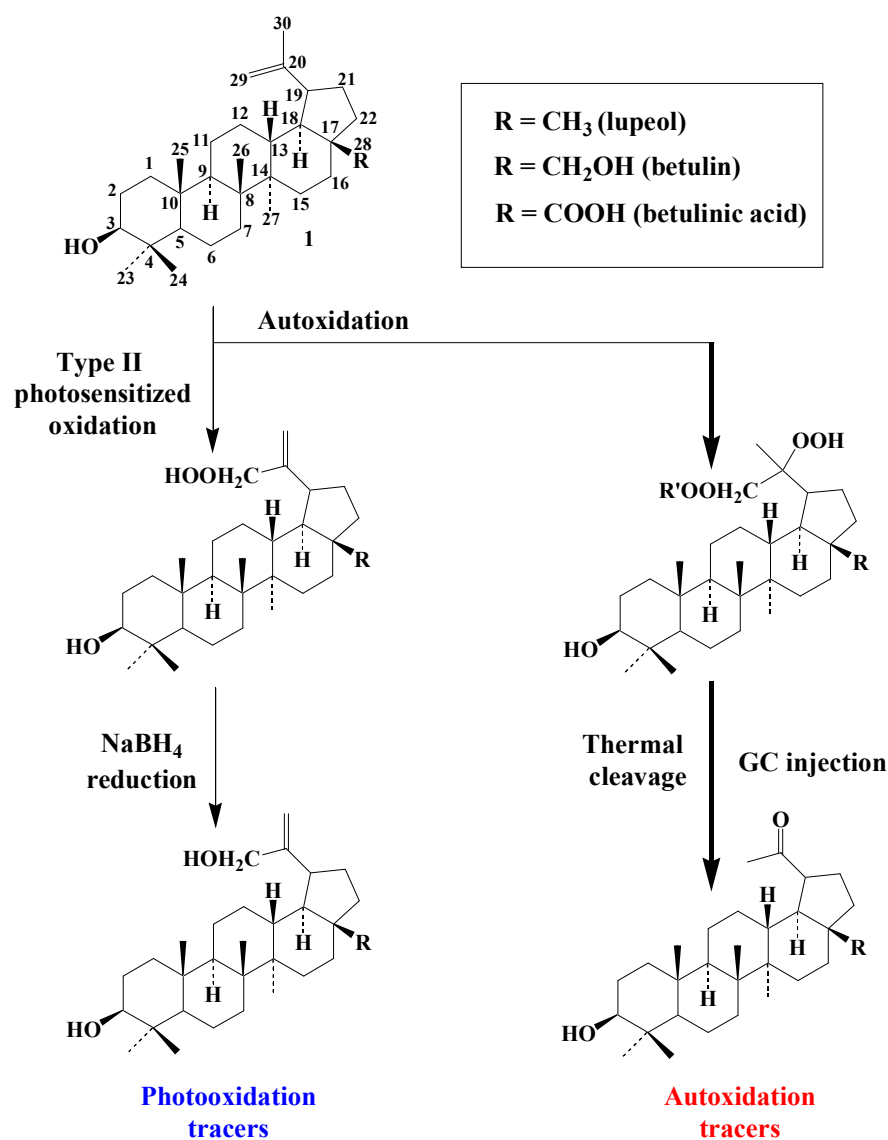
Figure 5. MRM chromatogram (m/z 199 \rightarrow 129, m/z 213 \rightarrow 129, m/z 329 \rightarrow 149 and m/z 343 \rightarrow 163) showing the presence of TMS derivatives of palmitoleic acid ($C_{16:1\omega 9}$) oxidation products in senescent cells of *Thalassiosira* sp. irradiated by sunlight.

3.45. Pentacyclic triterpenes

Pentacyclic triterpenes and their derivatives, which are widely found in angiosperms [58], are divided into three main classes, i.e. lupanes, oleananes and ursanes.

3.45.1. Lupanes

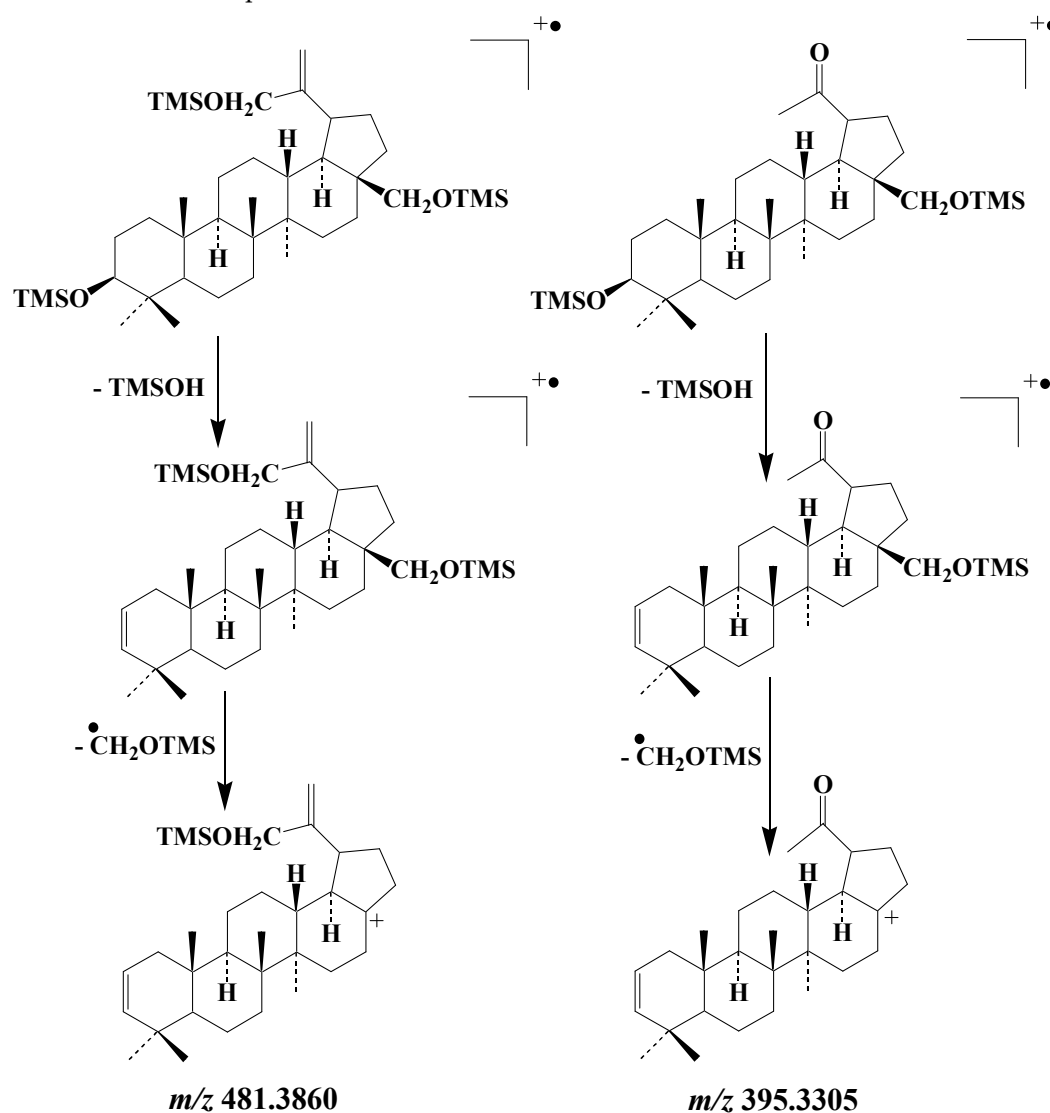
Type-II photooxidation and autooxidation of lupanes have so far only been studied for betulin [59], but the results obtained can be extended to lupeol or betulinic acid (the main triterpenoids with betulin of the lupane group). $^1\text{O}_2$ reacts slowly with the $\text{C}_{20}\text{-C}_{29}$ double bond of betulin and specifically produces lup-20(30)-ene-3 β ,28-diol-29-hydroperoxide, which can be quantified after NaBH_4 reduction in the form of lup-20(30)-ene-3 β ,28,29-triol (Scheme 7). Lup-20(30)-ene-3 β ,28,29-triol, lup-20(30)-ene-3 β ,29-diol (arising from lupeol) and lup-20(30)-ene-3 β ,29-diol-28-oic acid (arising from betulinic acid) constitute useful specific tracers of photooxidation of lupanes in angiosperms.



Scheme 7. Photooxidation and autooxidation of lupanes.

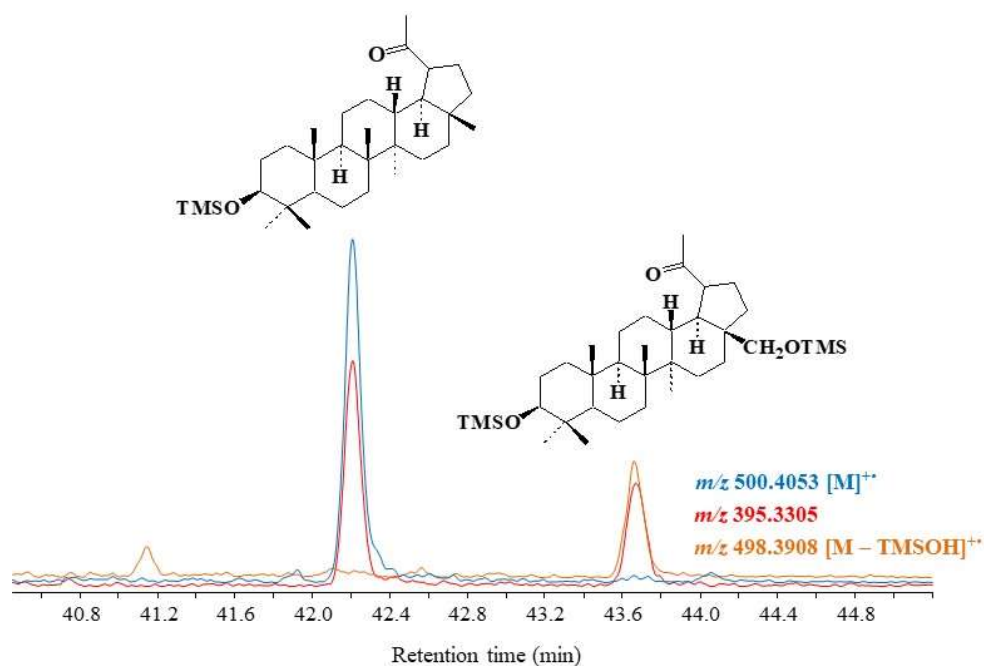
In contrast, the autoxidation of betulin mainly involves peroxy radical addition to the C₂₀-C₂₉ double bond and mainly affords a diperoxide that is unaffected by NaBH₄ reduction and converted to stable lupan-20-one-3β,28-diol during hot GC injection [59] (Scheme 7). Lupan-20-one-3β,28-diol, lupan-20-one-3β-ol (arising from lupeol) and lupan-20-one-3β-ol-28-oic acid (arising from betulinic acid) can be used as specific tracers of the autoxidation of lupanes in angiosperms [59,60].

The EI mass spectra of the TMS derivatives of lup-20(30)-ene-3β,28,29-triol and lupan-20-one-3β,28-diol exhibit intense fragment ions at *m/z* 481.3860 and *m/z* 395.3305, respectively, whose formation involves elimination of a neutral molecule of TMSOH and subsequent loss of the CH₂OTMS group borne by the carbon 28 [59] (Scheme 8). These fragment ions make good candidates for monitoring type-II photosensitized oxidation and autoxidation of betulin, respectively, in environmental samples. As the formation of these ions involves the loss of the group borne by carbon 28, they can be also used as tracers of the oxidation of lupeol and betulinic acid. Fig. 6 gives an example of the specific fragment ion at *m/z* 395.3305 applied for monitoring lupane autoxidation in environmental samples.



Scheme 8. Main EI fragmentations of the TMS derivatives of lup-20(30)-ene-3β,28,29-triol and lupan-20-one-3β,28-diol.

348



349

350

351

352

353

354

355

356

357

358

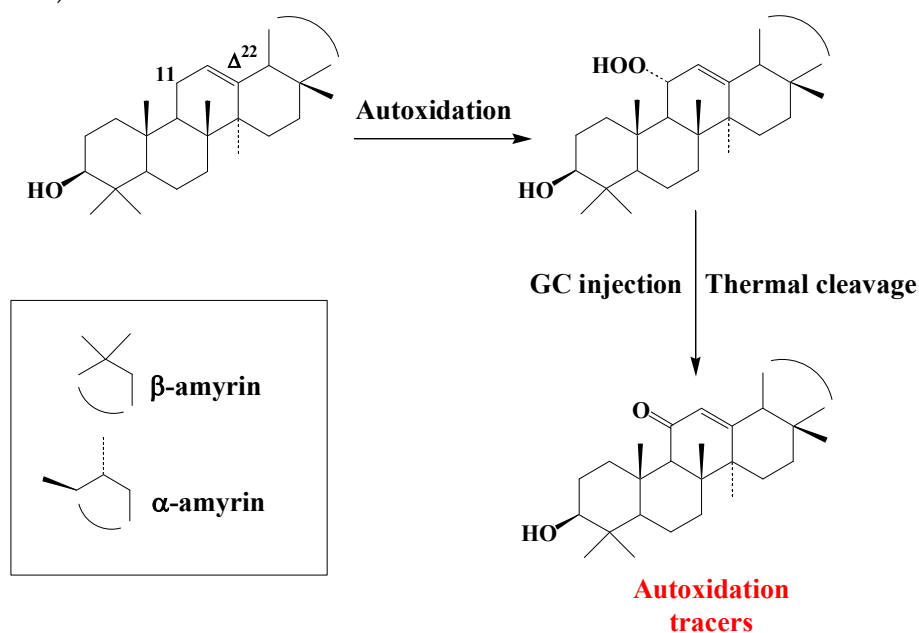
359

360

Figure 6. Partial TOF ion chromatograms (m/z 395.3305, 498.3908 and 500.4053) showing the presence of autoxidation products of lupeol and betulin in higher plant debris collected in the Rhône River.

3.45.2. Ursanes et oleanes

Studies on type II photosensitized oxidation and autoxidation of ursanes and oleanes have mainly focused on α - and β -amyrins [61]. α - and β -amyrins were found to be totally unaffected during photodegradation experiments, due to steric hindrance preventing 1O_2 reaction with their double bond [61]. Autoxidation of amyrins mainly involves hydrogen abstraction and specifically produces 11 α -hydroperoxyamyrins [61] (Scheme 9).



361

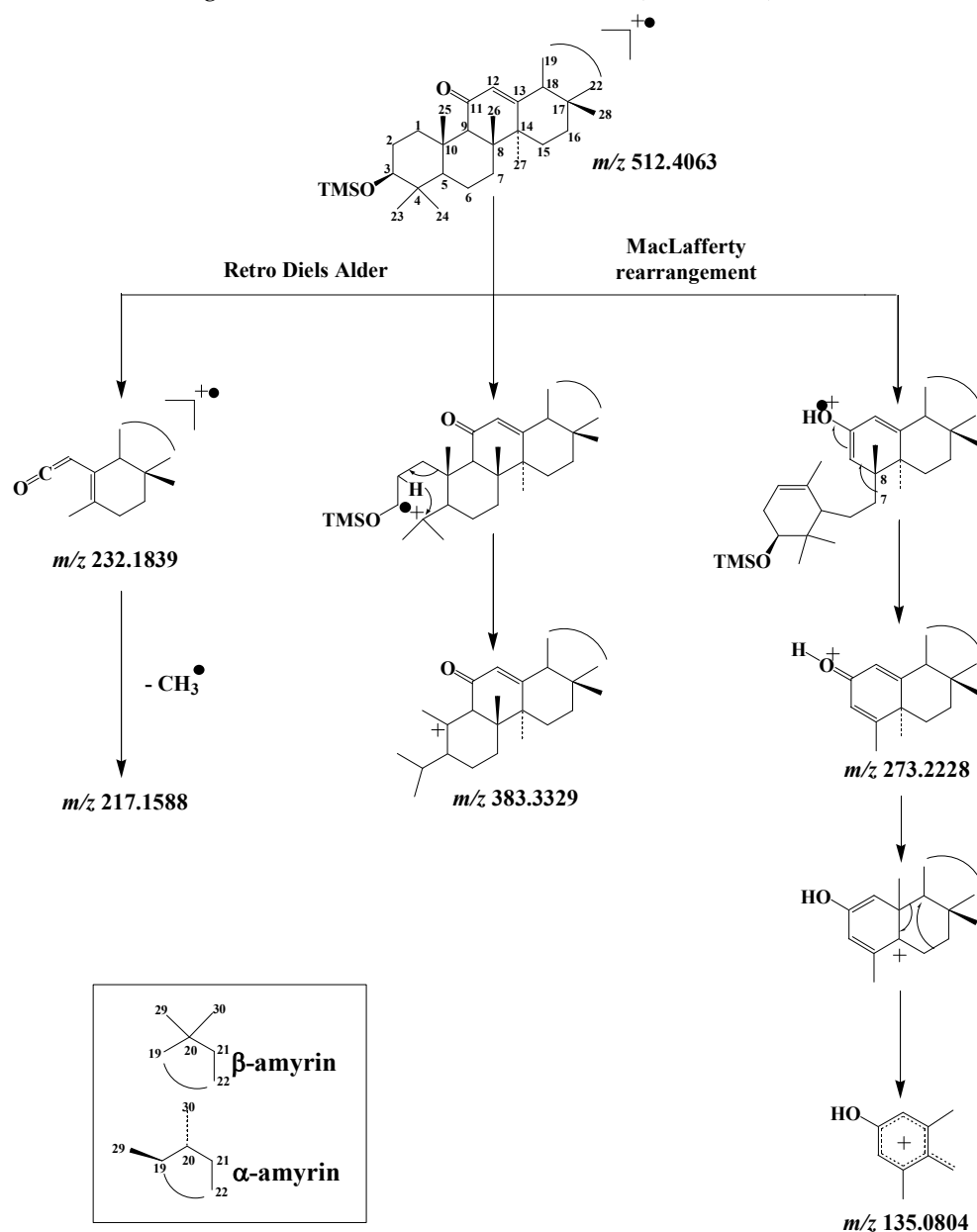
362

363

Scheme 9. Autoxidation of α - and β -amyrins.

These hydroperoxides, which appeared to be unaffected by NaBH₄ reduction, are thermally cleaved to the corresponding 11-oxoamyrins during GC or GC-MS analyses using hot injectors (Scheme 9). 11-Oxoamyrins are sufficiently stable and specific to serve as tracers of amyrin autoxidation in senescent angiosperms or environmental samples.

EI fragmentation of TMS derivatives of 11-oxoamyrins was recently studied [62] and found to involve: (i) retro-Diels-Alder cleavage of the unsaturated ring C leading to the formation of a fragment ion at m/z 232.1822, (ii) γ -hydrogen rearrangement of the ionized 11-keto group and subsequent cleavage of the 7–8 bond affording a well-stabilized fragment ion at m/z 273.2213, and (iii) a fragmentation pathway involving loss of the TMS group together with carbon atoms 1, 2 and 3 of the A ring after initial cleavage of the 3–4 bond [25] producing a fragment ion at m/z 383.3308 (Scheme 10). Subsequent fragmentation of the ion at m/z 273.2213 affords a strongly stabilized ion at m/z 135.0804 after migration of the methyl group 27 from carbon 14 to carbon 13 and concerted cleavage of the 13–18 and 15–16 bonds [63] (Scheme 10).



Scheme 10. Main EI mass fragmentation of TMS derivatives of 11-oxo-amyrins.

Note that after the loss of a methyl radical, a fragment ion at m/z 217.1588 can be formed from the fragment ion at m/z 232.1822 (Scheme 10). This fragmentation, which is more intense in the case of 11-oxo- β -amyrin due to the thermodynamically-favoured loss of a methyl radical from the tertiary carbon 20, may be useful for differentiating 11-oxo-amyrins.

Specific fragment ions at m/z 512.4063 [M]⁺, 383.3308, 273.2213 and 232.1822 appeared to be useful for GC-QTOF monitoring of TMS derivatives of 11-oxo-amyrins in environmental samples (see example given in Fig. 7A). MRM analyses using the transitions m/z 273 \rightarrow 135 and m/z 232 \rightarrow 217 also appeared to be well suited to the detection of traces of these compounds (see Fig. 7B).

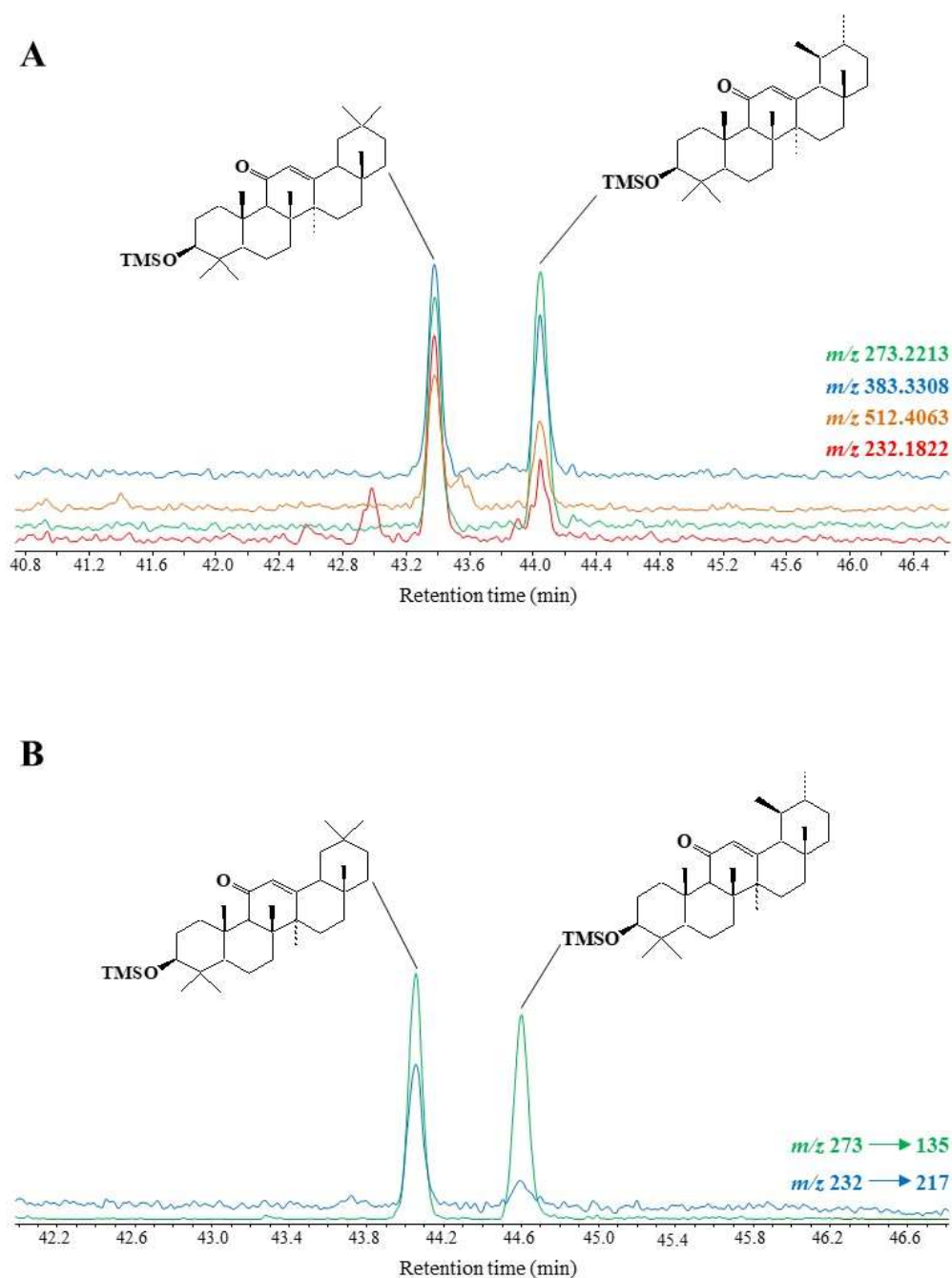
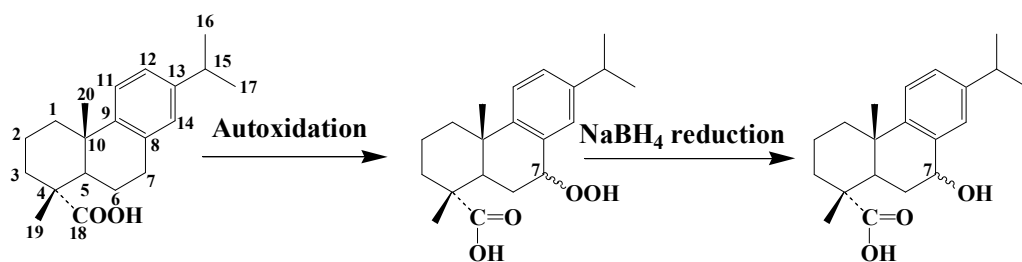


Figure 7. Partial TOF ion chromatogram (m/z 512.4063, 383.3308, 273.2213 and 232.1822) (A) and MRM chromatogram (m/z 273 \rightarrow 135 and m/z 232 \rightarrow 217) (B) showing the presence of oxidation products of amyrins in senescent leaves of *Quercus ilex*.

3.56. Dehydroabietic acid

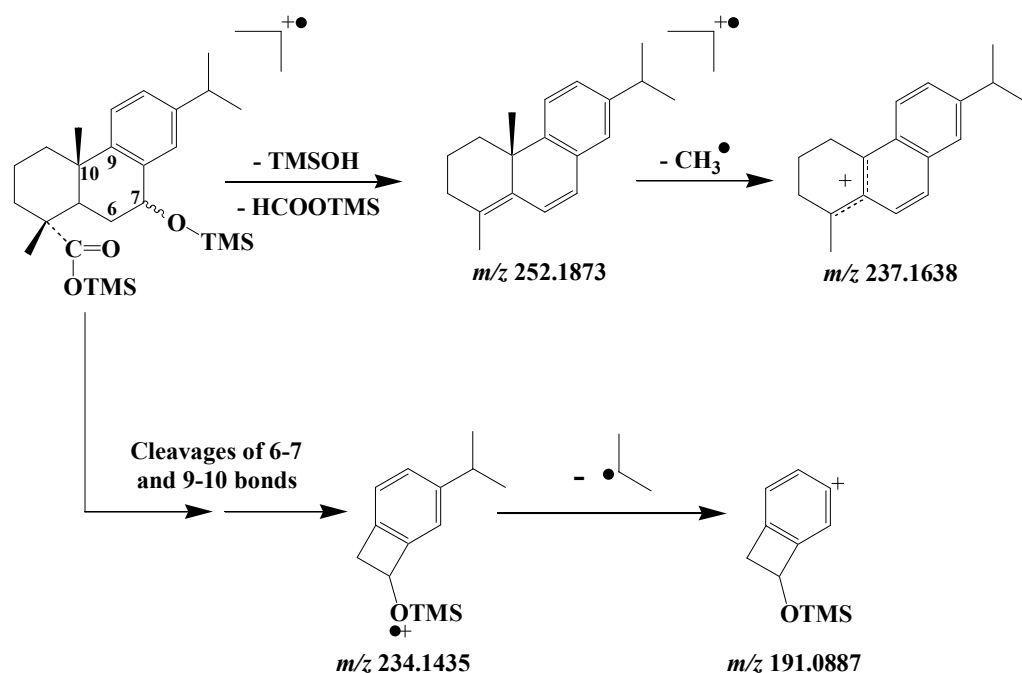
Dehydroabietic acid (8,11,13-abietatrien-18-oic acid), a component of conifers, has long been used as a tracer of gymnosperms [64,65]. Autoxidation of this compound involves hydrogen atom abstraction at the benzylic carbon atom 7 to give 7 α / β -hydroperoxydehydroabietic acids [66], which are reduced to the corresponding hydroxyacids during NaBH₄-reduction (Scheme 11). 7 α / β -hydroxydehydroabietic acids are useful tracers of dehydroabietic autoxidation in gymnosperms.



Autoxidation tracers

Scheme 11. Autoxidation of dehydroabietic acid.

EI mass spectra of TMS derivatives of 7 α / β -hydroxydehydroabietic acids exhibit intense fragment ions at m/z 191.0887, 234.1435 and 237.1638 [66]. The formation of the ion at m/z 237.1638 results from successive losses of neutral TMSOH and formate molecules and subsequent loss of a methyl radical (Scheme 12). The bicyclic fragment ion at m/z 234.1435 results from complex fragmentation processes involving cleavage of the 6-7 and 9-10 bonds [66] (Scheme 12); and it can readily lose an isopropyl radical to give a stable fragment ion at m/z 191.0887.



Scheme 12. Main EI mass fragmentations of TMS derivatives of 7 α / β -hydroxydehydroabietic acids.

Fragment ions at m/z 191.0887, 234.1435 and 237.1638 can be used in GC-QTOF analyses to characterize TMS derivatives of $7\alpha/\beta$ -hydroxydehydroabietic acids. However, MRM analyses using the highly specific transitions m/z 234 \rightarrow 191 and m/z 460 \rightarrow 417 [M – isopropyl group]⁺ emerged as better suited to detecting traces of these compounds in environmental samples (Fig. 8).

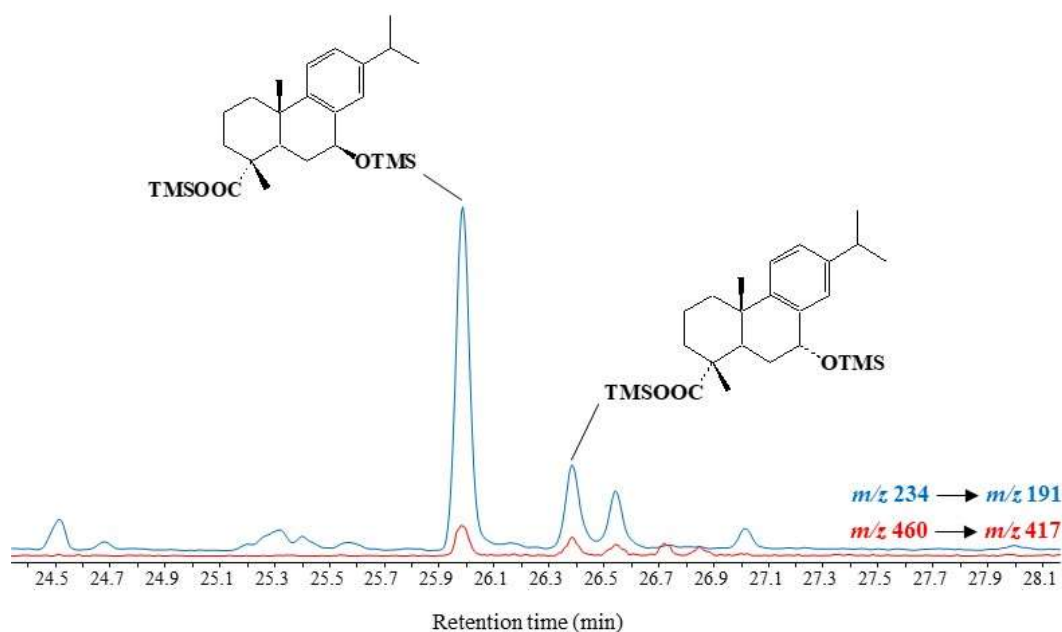
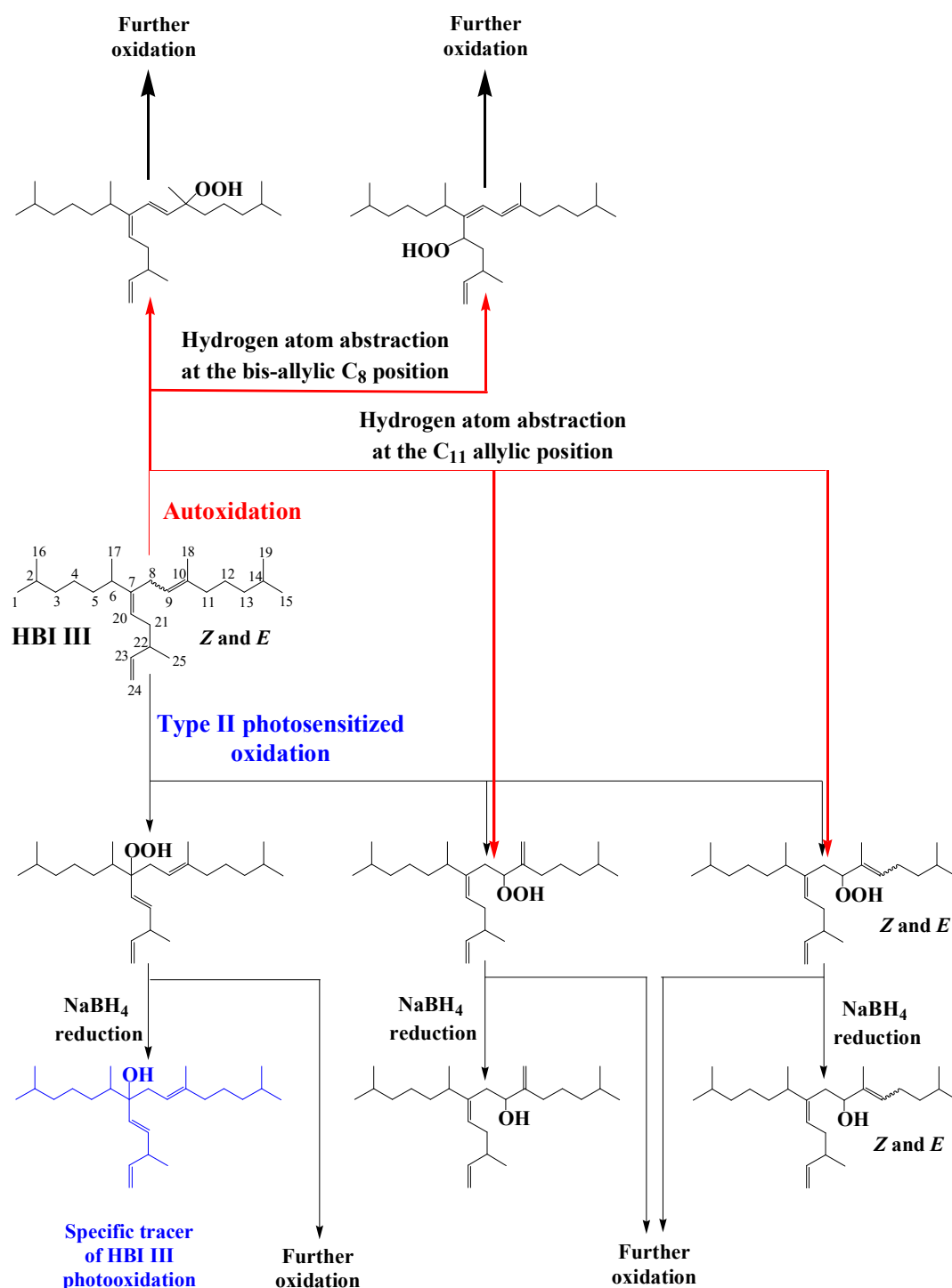


Figure 8. Partial MRM chromatogram (m/z 234 \rightarrow 191 and m/z 252 \rightarrow 237) showing the presence of autoxidation products of dehydroabietic acid in senescent needles of *Pinus halepensis*.

3.67. Highly branched isoprenoid (HBI) alkenes

HBI alkenes (exhibiting 1-6 double bonds) are produced by some marine and freshwater diatoms belonging to the *Berkeleya*, *Haslea*, *Navicula*, *Pleurosigma*, *Pseudosolenia* and *Rhizosolenia* genera [67,68]. During the senescence of these organisms, ¹O₂ attack is focused on the lesser sterically-hindered trisubstituted double bonds of these alkenes affording 2 or 4 allylic hydroperoxides according to the *E* or *Z* configuration of the double bond [69]. As an example, Scheme 13 shows type II photosensitized oxidation of *Z* and *E* isomers of HBI III, which are ubiquitous throughout the world's oceans [70]. In this case, ¹O₂ attack acts mainly on the C₉-C₁₀ double bond and to a lesser extent to the more sterically-hindered C₇-C₂₀ double bond affording 9- and 7-hydroperoxides, respectively, as the major oxidation products. Autoxidation processes also act very quickly on HBI III, producing numerous autoxidation products, but predominantly 9-hydroperoxides resulting from hydrogen atom abstraction at the allylic carbon 11 (Scheme 13) [71]. Indeed, the major oxidation pathway of this compound involves hydrogen abstraction at the bis-allylic C₈ position to afford conjugated dienes, which are particularly prone to peroxy radical additions and readily undergo copolymerization with oxygen (Scheme 13). Consequently, the 7-alcohol resulting from NaBH₄-reduction of the corresponding hydroperoxide could be used as specific tracer of type II photosensitized oxidation of HBI III (Scheme 13). However, the reduction products of 9-hydroperoxides will only be indicative of oxidation of this specific HBI alkene. Unfortunately, in the case of HBI alkenes (such as HBI III) possessing several trisubstituted double bonds, photooxidation and autoxidation products are unable to accumulate due to the involvement of fast secondary oxidation reactions [71]. All these tracers can thus only serve to give qualitative indications.

456

457
458

459

460

461

462

463

464

465

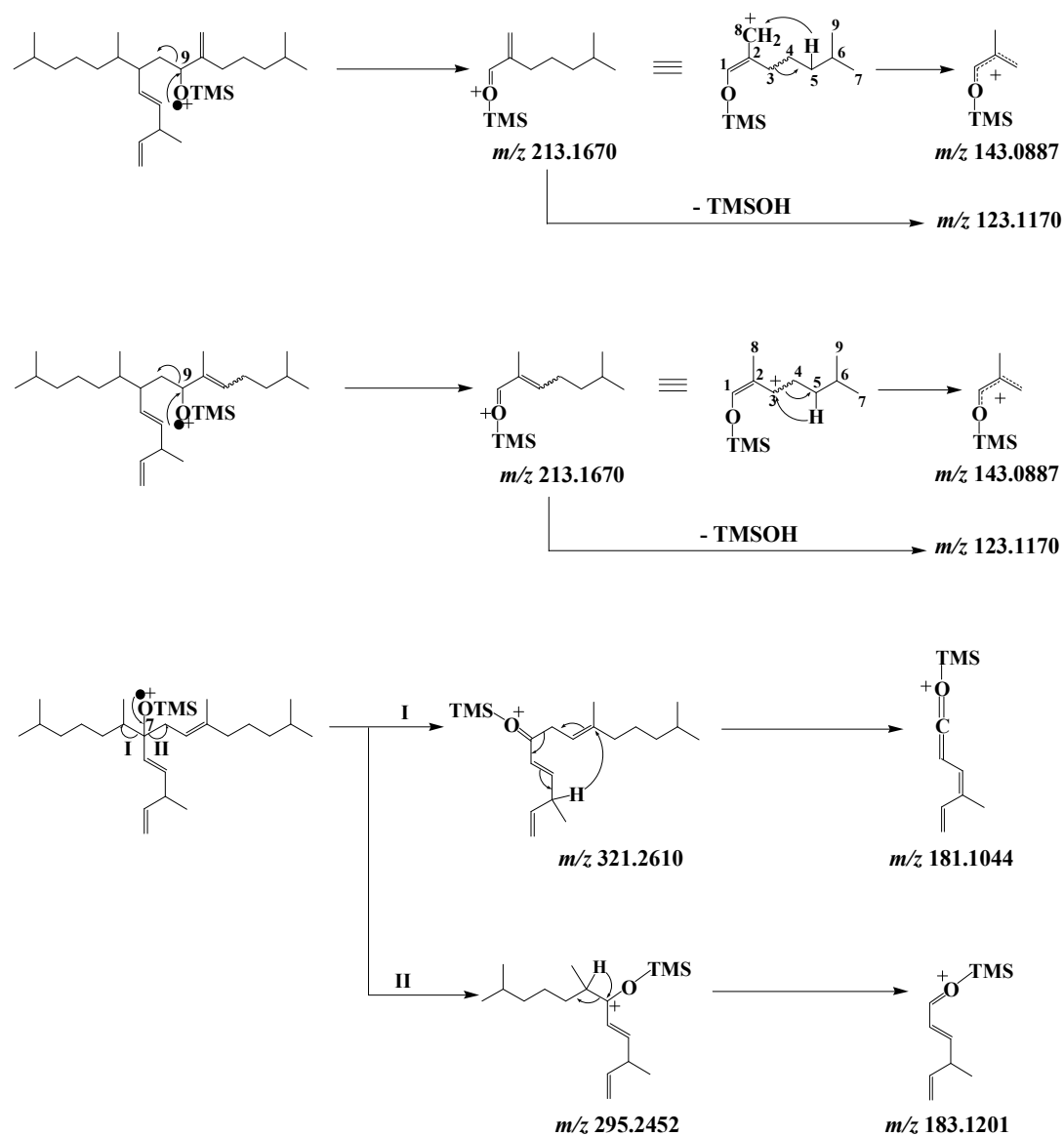
466

467

Scheme 13. Type II photosensitized oxidation and autoxidation of HBI III.

EI mass spectra of the TMS derivatives of the 9-alcohols resulting from HBI III oxidation exhibit an intense fragment ion at m/z 213.1670 corresponding to α -cleavage relative to the TMS ether group [72] (Scheme 14). This fragment ion can readily lose a neutral molecule of TMSOH to give a fragment ion at m/z 123.1170, or undergo a hydrogen transfer with concerted cleavage of the bond between carbon atoms 3 and 4, yielding a fragment ion at m/z 143.0887 (Fig. 22). In the case of the 7-alcohol, α -cleavage

relative to the TMS ether group affords two fragment ions at m/z 295.2452 and 321.2610, which are then cleaved in the α position relative to the ionized TMS ether group after hydrogen transfers to give fragment ions at m/z 183.1201 and 181.1044, respectively (Scheme 14).



Scheme 14. Main EI mass fragmentations of TMS derivatives of 9- and 7-alcohols resulting from oxidation of HBI III.

Oxidation products of HBI III were only characterizable in environmental samples in MRM mode using the m/z 213 \rightarrow 123, m/z 213 \rightarrow 143, m/z 295 \rightarrow 183 and m/z 321 \rightarrow 181 transitions [71–73]. An applied example is given in Fig. 9.

468
469
470
471
472

473
474
475
476
477
478
479
480
481
482
483
484

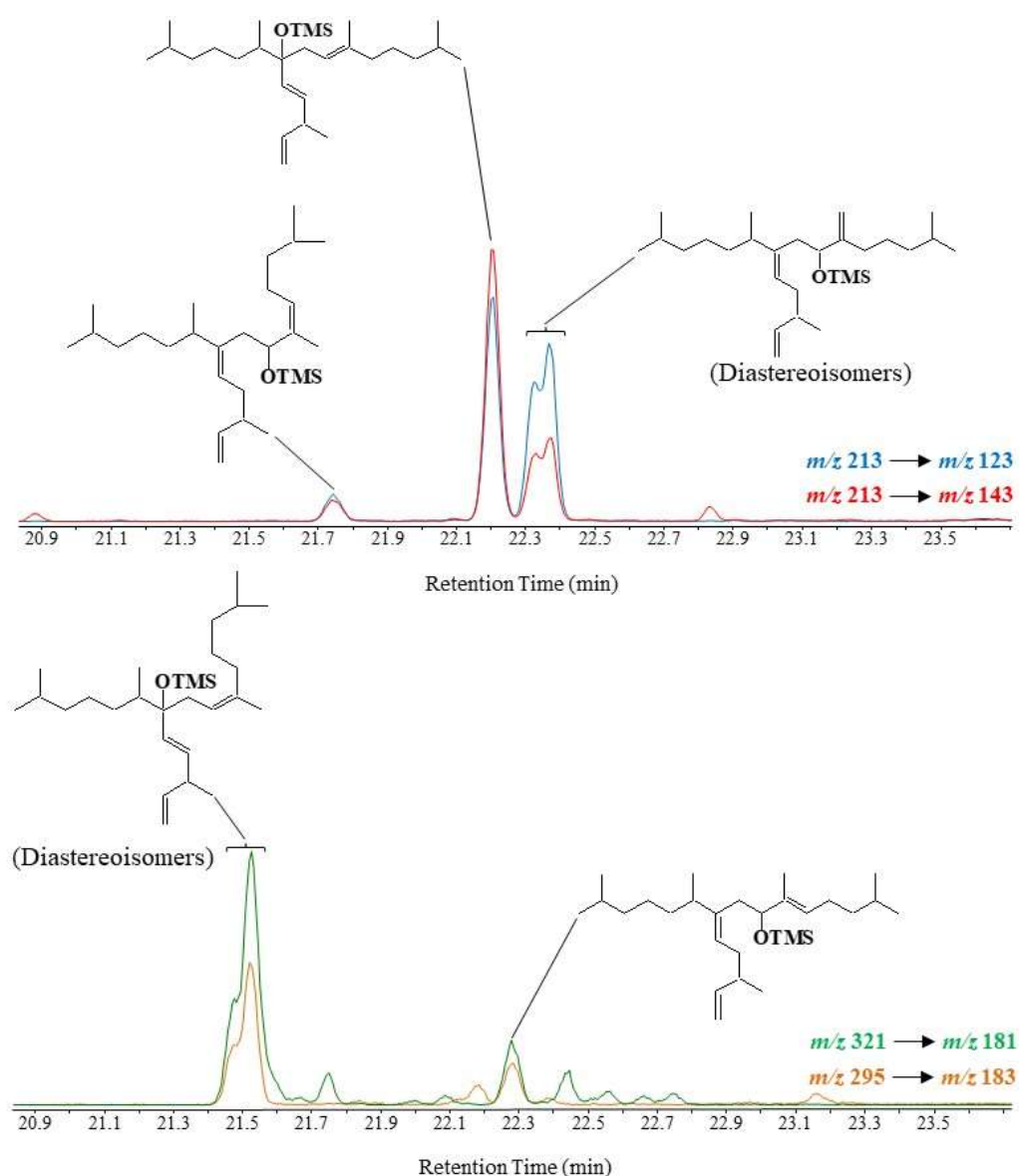


Figure 9. Partial MRM chromatograms (m/z 213 \rightarrow 123, m/z 213 \rightarrow 143, m/z 321 \rightarrow 181 and m/z 295 \rightarrow 183) showing the presence of oxidation products of HBI III in diatoms collected in Commonwealth Bay (Antarctic).

3.78. Alkenones

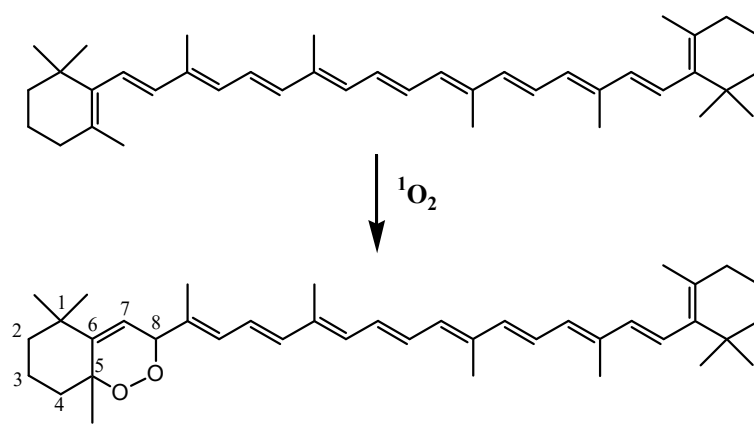
Alkenones are a class of mono-, di-, tri-, tetra- and penta-unsaturated C_{35} – C_{40} methyl and ethyl ketones, which are produced by certain haptophytes [74–78]. The unsaturation ratio of C_{37} alkenones, which is defined by the equation: $U_{37}^{K'} = [C_{37:2}] / ([C_{37:2}] + [C_{37:3}]$ (where $[C_{37:2}]$ and $[C_{37:3}]$ are the concentrations of di- and tri-unsaturated C_{37} methyl alkenones, respectively) varies positively with the growth temperature of the alga [79,80] and is thus now routinely used for paleotemperature reconstructions (e.g. [81,82]). Due to the *trans*- geometry of the alkenone double bonds [83], which is poorly reactive with 1O_2 [33], alkenones are not affected by type II photosensitized oxidation processes [84,85]. However, they are highly reactive to autoxidation processes [86]. Autoxidation of alkenone double bonds (separated by five or three methylene groups) affords six hydroperoxides as in the case of MUFAs (see chapter 3.3). Isomeric alkenediols resulting from $NaBH_4$ reduction of these oxidation products could make

485
486
487
488
489
490
491
492
493
494
495
496
497
498
499
500
501
502
503

504 very useful indicators of autoxidative alterations of the unsaturation ratio $U_{37}^{K'}$, but
505 unfortunately they fail to accumulate due to the subsequent oxidation of the other
506 double bonds [87]. Note that TMS derivatives of alkene-triols, tetraols or pentaols
507 obtained after NaBH₄ reduction and derivatization of secondary oxidation products of
508 di-, tri- or tetraunsaturated alkenones are too heavy and labile to be analyzed by GC-MS.
509 The characterization of alkenone autoxidation products in sediments or phytodetritus
510 with more adapted analytical techniques constitutes a very important challenge.

512 3.8 Carotenoids

513 Carotenoids, which are important antioxidant constituents of thylakoid
514 membranes, play special roles in the protection of tissues against damage caused by
515 light and oxygen [88]. These compounds can very efficiently quench ¹O₂ by energy
516 transfer (quenching), but also by chemical reaction (scavenging) [89]. They are also good
517 scavengers of ROS [90]. The attack of β-carotene by ¹O₂ affords β-carotene-5,8-
518 endoperoxide (Scheme 15) [91]. If this compound is generally considered as a useful
519 early signal of ¹O₂ production in plant leaves [92], it may be also formed during
520 autoxidation of β-carotene [93] and is clearly not stable enough to serve as a viable
521 environmental tracer. Unfortunately, the reaction of ¹O₂ and ROS with carotenoids
522 produces oxidation products that are not sufficiently stable and specific (production of
523 similar compounds by enzymatic processes) [93] to be used as unequivocal indicators of
524 type-II photosensitized oxidation or autoxidation of carotenoids in senescent
525 phototrophic organisms and environmental samples.



528

529 **Scheme 15.** Reaction of ¹O₂ with β-carotene.

531 4. Conclusion

532 In this review, a focus was given to the selection and characterization of stable
533 and specific tracers of photooxidation and autoxidation of lipid components
534 (chlorophyll phytol side-chain, Δ⁵-sterols, MUFAs, pentacyclic triterpenes and
535 dehydroabietic acid) of phototrophs. The author hope that it will contribute to a better
536 consideration of photooxidative and autoxidative processes almost ignored so far in the
537 literature when studying the degradation of autotrophic organisms in marine and
538 terrestrial environments.

539 The different oxidation products selected could be used as indicators of: (i)
540 oxidative stress of specific phototrophic organisms, (ii) paleoenvironmental changes of
541 the conditions of sedimentation (oxic or anoxic), (iii) abiotic alteration of paleoproxies in

oxic environments, (iv) environmental problems related to ozone depletion, and (v) abiotic degradation of permafrost released under the effect of global warming [94].

In the future, a special attention should be given to the detection of oxidation products of alkenones and HBI alkenes (possessing several trisubstituted double bonds) sufficiently stable and specific to act as tracers of oxidative alteration of these proxies in oxic environments (water column of oceans and oxic layer of sediments). MALDI-MS and IM-MS techniques, which allow simultaneous characterization of all molecular species in biological tissues and reduce sample preparation artifacts arising from extensive purification procedures [95], seem to be particularly well-adapted to this task.

NICI GC-MS, HPLC-MS and IM-MS techniques should be also used to give evidence of the presence of isoprostanoïds resulting from PUFA oxidation in environmental samples. Due to the very high reactivity of PUFA towards photooxidation and autoxidation processes, such compounds could be very sensitive tracers of the early stages of oxidative damages.

Funding: The author thanks the Centre National de la Recherche Scientifique (CNRS) and Aix-Marseille University for providing financial support over the years. Thanks are also due to the FEDER project OCEANOMED (No. 1166-39417) for the funding of the GC-QTOF and GC-MS/MS employed.

Acknowledgements: Special thanks are due to Dr. C. Aubert for the many friendly and fruitful discussions we have had over the years concerning the mechanisms of lipid fragmentation upon electron impact. Thanks are also due to three anonymous reviewers for their useful and constructive comments.

Institutional Review Board Statement: Not applicable.

Informed Consent Statement: Not applicable.

Data Availability Statement: Not applicable.

Conflict of Interest: The author declare no conflict of interest.

References

1. Shimakawa, G.; Matsuda, Y.; Nakajima, K.; Tamoi, M.; Shigeoka, S.; Miyake, C. Diverse strategies of O₂ usage for preventing photo-oxidative damage under CO₂ limitation during algal photosynthesis. *Scientific Reports* **2017**, *7*, 41022.
2. Harwood, J.L.; Russell, N.J. *Lipids in Plants and Microbes*; Springer: Dordrecht, Germany, 1984; pp. 7-32.
3. Jónasdóttir, S.H. Fatty acid profiles and production in marine phytoplankton. *Marine Drugs* **2019**, *17*, 151.
4. Ben-Amotz, A.; Tornabene, T.G.; Thomas, W.H. Chemical profile of selected species of microalgae with emphasis on lipids 1. *Journal of Phycology* **1985**, *21*, 72-81.
5. Volkman, J.K. Lipid markers for marine organic matter. *The Handbook of Environmental Chemistry* **2006**, *2*, 27-70.
6. Parrish, C.C. Lipids in marine ecosystems. *International Scholarly Research Notices* **2013**, 604045.
7. Guo, J.; Glendell, M.; Meersmans, J.; Kirkels, F.; Middelburg, J.J.; Peterse, F. Assessing branched tetraether lipids as tracers of soil organic carbon transport through the Carminowe Creek Catchment (Southwest England). *Biogeosciences* **2020**, *17*, 3183-3201.
8. Rontani, J.-F., 2012. Photo- and Free Radical-Mediated Oxidation of Lipid Components during the Senescence of Phototrophic Organisms. In *Senescence*, Nagata Tetsuji (Ed.); Intech: Rijeka, Croatia, 2012; pp. 3-31.
9. Rontani, J.-F.; Belt, S.T. Photo- and autoxidation of unsaturated algal lipids in the marine environment: an overview of processes, their potential tracers, and limitations. *Organic Geochemistry* **2020**, *139*, 103941.
10. Marchand, D.; Rontani, J.-F. Characterisation of photo-oxidation and autoxidation products of phytoplanktonic monounsaturated fatty acids in marine particulate matter and recent sediments. *Organic Geochemistry* **2001**, *32*, 287-304.

- 592 **11.** Xia, W.; Budge, S.M. Techniques for the analysis of minor lipid oxidation products derived from triacylglycerols: epoxides,
593 alcohols, and ketones. *Comprehensive Reviews in Food Science and Food Safety* **2017**, *16*, 735-758.
- 594 **12.** Xu, L.; Yu, X.; Li, M.; Chen, J.; Wang, X. Monitoring oxidative stability and changes in key volatile compounds in edible oils
595 during ambient storage through HS-SPME/GC-MS. *International journal of food properties* **2017**, *20*, S2926-S2938.
- 596 **10-13.** Barden, A.; Mori, T.A. GC-MS analysis of lipid oxidation products in blood, urine, and tissue samples. In *Clinical Metabolomics*,
597 Humana Press, New York, USA, 2018; pp. 283-292.
- 598 **14.** Koek, M.M.; Jellema, R.H.; van der Greef, J.; Tas, A.C.; Hankemeier, T. Quantitative metabolomics based on gas chromatography
599 mass spectrometry: status and perspectives. *Metabolomics* **2011**, *7*, 307-328.
- 600 **15.** Frankel, E.N. *Lipid oxidation*; Woodhead Publishing: Cambridge, U.K., 2014; pp. 129-161.
- 601 **16.** Schick, D.; Link, K.; Schwack, W.; Granvogl, M.; Oellig, C. Analysis of mono-, di-, triacylglycerols, and fatty acids in food emul-
602 sifiers by high-performance liquid chromatography-mass spectrometry. *European Food Research and Technology* **2021**, *247*, 1023-
603 1034.
- 604 **17.** Han, E.C.; Lee, Y.S.; Liao, W.S.; Liu, Y.C.; Liao, H.Y.; Jeng, L.B. Direct tissue analysis by MALDI-TOF mass spectrometry in
605 human hepatocellular carcinoma. *Clinica Chimica Acta*, **2011**, *412*, 230-239.
- 606 **18.** Leopold, J.; Popkova, Y.; Engel, K.M.; Schiller, J. Recent developments of useful MALDI matrices for the mass spectrometric
607 characterization of lipids. *Biomolecules*, **2018**, *8*, 173.
- 608 **19.** Paglia, G.; Kliman, M.; Claude, E.; Geromanos, S.; Astarita, G. Applications of ion-mobility mass spectrometry for lipid analysis.
609 *Analytical and bioanalytical chemistry*, **2015**, *407*, 4995-5007.
- 610 **20.** Leaptrot, K.L.; May, J.C.; Dodds, J.N.; McLean, J.A. Ion mobility conformational lipid atlas for high confidence lipidomics. *Na-
611 ture communications*, **2019**, *10*, 1-9.
- 612 **11-21.** Merx, D.W.; Hong, G.S.; Ermacora, A.; Van Duynhoven, J.P. Rapid quantitative profiling of lipid oxidation products in a food
613 emulsion by ¹H NMR. *Analytical chemistry*, **2018**, *90*, 4863-4870.
- 614 **12-22.** He, P.; Aga, D.S. Comparison of GC-MS/MS and LC-MS/MS for the analysis of hormones and pesticides in surface waters:
615 advantages and pitfalls. *Analytical Methods* **2019**, *11*, 1436-1448.
- 616 **13-23.** Pierce, A.E. *Silylation of Organic Compounds*. Pierce Chemical Company: Rockford Illinois, 1982; pp. 72-215.
- 617 **14-24.** Evershed, R. Biomolecular archaeology and lipids. *World Archaeology* **1993**, *25*, 74-93.
- 618 **15-25.** Goad, L.J.; Akihisa, T. Mass Spectrometry of Sterols. In *Analysis of Sterols*, Goad, L.J. and Akihisa, T. (Eds.); Springer: Dordrecht,
619 Germany, 1997; pp. 152-196.
- 620 **16-26.** Harvey, D.J.; Vouros, P. Mass spectrometric fragmentation of trimethylsilyl and related alkylsilyl derivatives. *Mass Spectrom-
621 etry Reviews* **2020**, *39*, 105-211.
- 622 **17-27.** Foote, C.S. Photosensitized Oxidation and Singlet Oxygen: Consequences in Biological Systems. In *Free Radicals in Biology*,
623 Pryor, W.A. (Ed.); Academic Press: New York, United States, 1976; pp. 85-133.
- 624 **18-28.** Knox, J.P.; Dodge, A.D. Singlet oxygen and plants. *Phytochemistry* **1985**, *24*, 889-896.
- 625 **19-29.** Halliwell, B. Oxidative damage, lipid peroxidation and antioxidant protection in chloroplasts. *Chemistry and Physics of lipids*
626 **1987**, *44*, 327-340.
- 627 **20-30.** Nelson, J.R. Rates and possible mechanism of light-dependent degradation of pigments in detritus derived from phytoplank-
628 ton. *Journal of Marine Research* **1993**, *51*, 155-179.
- 629 **21-31.** Merzlyak, M.N.; Hendry, G.A.F. Free radical metabolism, pigment degradation and lipid peroxidation in leaves during senes-
630 cence. *Proceedings of the Royal Society of Edinburgh* **1994**, *102B*, 459-471.
- 631 **22-32.** Glaeser, J.; Nuss, A.M.; Berghoff, B.A.; Klug, G. Singlet oxygen stress in microorganisms. *Advances in microbial physiology* **2011**,
632 *58*, 141-173.
- 633 **23-33.** Hurst, J.R.; Wilson, S.L.; Schuster, G.B. The ene reaction of singlet oxygen: kinetic and product evidence in support of a
634 peroxide intermediate. *Tetrahedron* **1985**, *41*, 2191-2197.
- 635 **24-34.** Krumova, K.; Cosa, G. Overview of Reactive Oxygen Species. In *Singlet Oxygen: Applications in Biosciences and Nanosciences*,
636 Santi, N. and Flors C. (Eds.); The Royal Society of Chemistry: London, U.K.; volume 1, pp. 1-21.
- 637 **25-35.** Schaich, K.M. Lipid Oxidation: Theoretical Aspects. In *Bailey's Industrial Oil and Fat Products*, Shahidi, F. (Ed.); John Wiley &
638 Sons: Chichester, U.K.; 2005; pp. 269-355.
- 639 **26-36.** Fossey, J.; Lefort, D.; Sorba, J. *Free Radicals in Organic Chemistry*. John Wiley & Sons: Chichester, U.K.; 1995; pp. 191-200.
- 640 **27-37.** Girotti, A.W. Lipid hydroperoxide generation, turnover, and effector action in biological systems. *Journal of Lipid Research* **1998**,
641 *39*, 1529-1542.
- 642 **28-38.** Rontani, J.-F.; Rabourdin, A.; Marchand, D.; Aubert, C. Photochemical oxidation and autoxidation of chlorophyll phytyl side
643 chain in senescent phytoplanktonic cells: potential sources of several acyclic isoprenoid compounds in the marine environment.
644 *Lipids* **2003**, *38*, 241-254.
- 645 **29-39.** Rontani, J.-F.; Cuny, P.; Grossi, V. Photodegradation of chlorophyll phytyl chain in senescent leaves of higher plants. *Phyto-
646 chemistry* **1996**, *42*, 347-351.
- 647 **30-40.** Cuny, P.; Rontani, J.-F. On the widespread occurrence of 3-methylidene-7,11,15-trimethylhexadecan-1,2-diol in the marine
648 environment: a specific isoprenoid marker of chlorophyll photodegradation. *Marine Chemistry* **1999**, *65*, 155-165.

- 649 [31-41](#). Rontani, J.-F.; Aubert, C. Characterization of isomeric allylic diols resulting from chlorophyll phytyl side-chain photo- and
650 autoxidation by electron ionization gas chromatography/mass spectrometry. *Rapid Communications in Mass Spectrometry* **2005**,
651 *19*, 637-646.
- 652 [32-42](#). Rontani, J.-F.; Galeron, M.-A. Autoxidation of chlorophyll phytyl side chain in senescent phototrophic organisms: a potential
653 source of isophytol in the environment. *Organic Geochemistry* **2016**, *97*, 35-40.
- 654 [33-43](#). Kulig, M.J.; Smith, L.L. Sterol metabolism. XXV. Cholesterol oxidation by singlet molecular oxygen. *Journal of Organic Chemistry*
655 **1973**, *38*, 3639-3642.
- 656 [34-44](#). Korytowski, W.; Bachowski, G.J.; Girotti, A.W. Photoperoxidation of cholesterol in homogeneous solution, isolated mem-
657 branes, and cells: comparison of the 5 α - and 6 β -hydroperoxides as indicators of singlet oxygen intermediacy. *Photochemistry and*
658 *Photobiology* **1992**, *56*, 1-8.
- 659 [35-45](#). Christodoulou, S.; Marty, J.-C.; Miquel, J.-C.; Volkman, J.K.; Rontani, J.-F. Use of lipids and their degradation products as
660 biomarkers for carbon cycling in the northwestern Mediterranean Sea. *Marine Chemistry* **2009**, *113*, 25-40.
- 661 [36-46](#). Rontani, J.-F.; Zabeti, N.; Wakeham, S.G. The fate of marine lipids: biotic vs. abiotic degradation of particulate sterols and
662 alkenones in the northwestern Mediterranean Sea. *Marine Chemistry* **2009**, *113*, 9-18.
- 663 [37-47](#). Smith, L.L. Cholesterol autoxidation 1981-1986. *Chemistry and Physics of Lipids* **1981**, *44*, 87-125.
- 664 [38-48](#). Morrissey, P.A.; Kiely, M. Oxysterols: formation and biological function. *Advanced Dairy Chemistry* **2006**, *2*, 641-674.
- 665 [39-49](#). Harvey, D.J.; Vouros, P. Influence of the 6-trimethylsilyl group on the fragmentation of the trimethylsilyl derivatives of some
666 6-hydroxy- and 3,6-dihydroxy-steroids and related compounds. *Biomedical Mass Spectrometry* **1979**, *6*, 135-143.
- 667 [40-50](#). Rontani, J.-F.; Charrière, B.; Sempéré, R.; Doxaran, D.; Vaultier, F.; Vonk, J.E.; Volkman, J.K. Degradation of sterols and terri-
668 genous organic matter in waters of the Mackenzie Shelf, Canadian Arctic. *Organic Geochemistry* **2014**, *75*, 61-73.
- 669 [41-51](#). Frankel, E.N. *Lipid Oxidation*. The Oily Press: Dundee, U.K., 1998; pp. 23-41.
- 670 [52](#). Rontani, J.-F.; Cuny, P.; Grossi, V. Identification of a "pool" of lipid photoproducts in senescent phytoplanktonic cells. *Organic*
671 *Geochemistry* **1998**, *29*, 1215-1225.
- 672 [53](#). [Vigor, C.; Bertrand-Michel, J.; Pinot, E.; Oger, C.; Vercauteren, J.; Le Faouder, P.; Galano, J.M.; Lee, J.C.-Y.; Durand, T. Non-](#)
673 [enzymatic lipid oxidation products in biological systems: assessment of the metabolites from polyunsaturated fatty acids. *Journal of Chromatography B* **2014**, *964*, 65-78.](#)
- 674 [42-54](#). [Imbusch, R.; Mueller, M.J. Formation of isoprostane F2-like compounds \(phytoprostanes F1\) from \$\alpha\$ -linolenic acid in plants. *Free Radical Biology and Medicine* **2000**, *28*, 720-726.](#)
- 675 [43-55](#). Frankel, E.N.; Neff, W.E.; Bessler, T.R. Analysis of autoxidized fats by gas chromatography-mass spectrometry: V. Photosen-
676 sitized oxidation. *Lipids* **1979**, *14*, 961-967.
- 677 [44-56](#). Porter, N.A.; Caldwell, S.E.; Mills, K.A. Mechanisms of free radical oxidation of unsaturated lipids. *Lipids* **1995**, *30*, 277-290.
- 680 [45-57](#). Christodoulou, S.; Joux, F.; Marty, J.-C.; Sempéré, R.; Rontani, J.-F. Comparative study of UV and visible light induced degra-
681 dation of lipids in non-axenic senescent cells of *Emiliania huxleyi*. *Marine Chemistry* **2010**, *119*, 139-152.
- 682 [46-58](#). Jäger, S.; Trojan, H.; Kopp, T.; Laszczyk, M.N.; Scheffler, A. Pentacyclic triterpene distribution in various plants-rich sources
683 for a new group of multi-potent plant extracts. *Molecules* **2009**, *14*, 2016-2031.
- 684 [47-59](#). Galeron, M.-A.; Volkman, J.K.; Rontani, J.-F. Oxidation products of betulin: new tracers of abiotic degradation of higher plant
685 material in the environment. *Organic Geochemistry* **2016**, *91*, 31-42.
- 686 [48-60](#). Rontani J.-F. *Lipid Oxidation Products: Useful Tools for Monitoring Photo- and Autoxidation in Phototrophs*. Cambridge Scholar
687 Publishing: Newcastle upon Tyne, U.K., 2021, pp. 51-70.
- 688 [49-61](#). Galeron, M.-A.; Vaultier, F.; Rontani, J.-F. Oxidation products of α - and β -amyrins: potential tracers of abiotic degradation of
689 vascular-plant organic matter in aquatic environments. *Environmental Chemistry* **2016**, 15237.
- 690 [50-62](#). Rontani, J.-F.; Charrière, B.; Menniti, C.; Aubert, D.; Aubert, C. Electron ionization mass spectrometry fragmentation and mul-
691 tiple reaction monitoring quantification of autoxidation products of α - and β -amyrins in natural samples. *Rapid Communications*
692 *in Mass Spectrometry* **2018**, *32*, 1599-1607.
- 693 [51-63](#). Budzikiewicz, H.; Wilson, J.M.; Djerassi, C. Mass spectrometry in structural and stereochemical problems. XXXII.1 Pentacyclic
694 triterpenes. *Journal of the American Chemical Society* **1963**, *85*, 3688-3699.
- 695 [52-64](#). Brassell, S.C.; Eglinton, G.; Maxwell, J.R. The geochemistry of terpenoids and steroids. *Biochemical Society Transactions* **1983**, *1*,
696 575-586.
- 697 [53-65](#). Otto, A.; Simoneit, B.R.T.; Rember, W.C. Conifer and angiosperm biomarkers in clay sediments and fossil plants from the
698 Miocene Clarkia Formation, Idaho, USA. *Organic Geochemistry* **2005**, *36*, 907-922.
- 699 [54-66](#). Rontani, J.-F.; Aubert, C.; Belt, S.T. EIMS Fragmentation pathways and MRM quantification of 7 α / β -hydroxy-dehydroabietic
700 acid TMS derivatives. *Rapid Communications in Mass Spectrometry* **2018**, *26*, 1606-1616.
- 701 [55-67](#). Belt, S.T.; Müller, J. The Arctic sea ice biomarker IP₂₅: a review of current understanding, recommendations for future research
702 and applications in palaeo sea ice reconstructions. *Quaternary Science Reviews* **2013**, *79*, 9-25.
- 703 [56-68](#). Belt, S.T. Source-specific biomarkers as proxies for Arctic and Antarctic sea ice. *Organic Geochemistry* **2018**, *125*, 277-298.
- 704 [57-69](#). Schulte-Elte, K.H.; Muller, B.L.; Pamingle, H. Photooxygenation of 3, 3-dialkylsubstituted allyl alcohols. Occurrence of *syn*
705 preference in the ene addition of ¹O₂ at *E/Z*-isomeric allyl alcohols. *Helvetica Chimica Acta* **1979**, *62*, 816-829.

- 706 [58-70](#). Belt, S.T.; Brown, T.A.; Smik, L.; Tatarek, A.; Wiktor, J.; Stowasser, G.; Husum, K. Identification of C₂₅ highly branched isoprenoid (HBI) alkenes in diatoms of the genus *Rhizosolenia* in polar and sub-polar marine phytoplankton. *Organic Geochemistry* **2017**, *110*, 65-72.
- 707
- 708
- 709 [59-71](#). Rontani, J.-F.; Belt, S.T.; Brown, T.A.; Vaultier, F.; Mundy, C.J. Sequential photo-and autoxidation of diatom lipids in Arctic sea ice. *Organic geochemistry* **2014**, *77*, 59-71.
- 710
- 711 [60-72](#). Rontani, J.-F.; Belt, S.T.; Brown, T.A.; Aubert, C. Electron ionization mass spectrometry fragmentation pathways of trimethylsilyl derivatives of isomeric allylic alcohols derived from HBI alkene oxidation. *Rapid Communications in Mass Spectrometry* **2014**, *28*, 1937-1947.
- 712
- 713
- 714 [61-73](#). Rontani, J.-F.; Smik, L.; Belt, S.T.; Vaultier, F.; Armbrrecht, L.; Leventer, A.; Armand, L.K. Abiotic degradation of highly branched isoprenoid alkenes and other lipids in the water column off East Antarctica. *Marine Chemistry* **2019**, *210*, 34-47.
- 715
- 716 [62-74](#). Volkman, J.K.; Eglinton, G.; Corner, E.D.; Forsberg, T.E.V. Long-chain alkenes and alkenones in the marine coccolithophorid *Emiliania huxleyi*. *Phytochemistry* **1980**, *19*, 2619-2622.
- 717
- 718 [63-75](#). Volkman, J.K.; Barrett, S.M.; Blackburn, S.I.; Sikes, E.L. Alkenones in *Gephyrocapsa oceanica*: implications for studies of paleoclimate. *Geochimica et Cosmochimica Acta* **1995**, *59*, 513-520.
- 719
- 720 [64-76](#). Marlowe, I.T.; Green, J.C.; Neal, A.C.; Brassell, S.C.; Eglinton, G.; Course, P.A. Long chain (n-C₃₇-C₃₉) alkenones in the Prymnesiophyceae. Distribution of alkenones and other lipids and their taxonomic significance. *British Phycological Journal* **1984**, *19*, 203-216.
- 721
- 722
- 723 [65-77](#). Prahl, F.G.; Mix, A.C.; Sparrow, M.A. Alkenone paleothermometry: biological lessons from marine sediment records off western South America. *Geochimica et Cosmochimica Acta* **2006**, *70*, 101-117.
- 724
- 725 [66-78](#). Jaraula, C.M.; Brassell, S.C.; Morgan-Kiss, R.M.; Doran, P.T.; Kenig, F. Origin and tentative identification of tri- to penta-unsaturated ketones in sediments from Lake Fryxell, East Antarctica. *Organic Geochemistry* **2010**, *41*, 386-397.
- 726
- 727 [67-79](#). Prahl, F.G.; Wakeham, S.G. Calibration of unsaturation patterns in long-chain ketone compositions for palaeotemperature assessment. *Nature* **1987**, *330*, 367-369.
- 728
- 729 [68-80](#). Prahl, F.G.; Muehlhausen, L.A.; Zahnle, D.L. Further evaluation of long-chain alkenones as indicators of paleoceanographic conditions. *Geochimica et Cosmochimica Acta* **1988**, *52*, 2303-2310.
- 730
- 731 [69-81](#). Brassell, S.C. Applications of biomarkers for delineating marine paleoclimatic fluctuations during the Pleistocene. *Organic Geochemistry* **1993**, 699-738.
- 732
- 733 [70-82](#). Müller, P.J.; Kirst, G.; Ruhland, G.; Von Storch, I.; Rosell-Melé, A. Calibration of the alkenone paleotemperature index $U_{37}^{K'}$ based on core-tops from the eastern South Atlantic and the global ocean (60° N-60° S). *Geochimica et Cosmochimica Acta* **1998**, *62*, 1757-1772.
- 734
- 735
- 736 [71-83](#). Reckha J.A.; Maxwell, J.R. Characterisation of alkenone temperature indicators in sediments and organisms. *Organic Geochemistry* **1988**, *13*, 727-734.
- 737
- 738 [72-84](#). Rontani, J.-F.; Cuny, P.; Grossi, V.; Beker, B. Stability of long-chain alkenones in senescing cells of *Emiliania huxleyi*: effect of photochemical and aerobic microbial degradation on the alkenone unsaturation ratio $U_{37}^{K'}$. *Organic Geochemistry* **1997**, *26*, 503-509.
- 739
- 740
- 741 [73-85](#). Mouzdahir, A.; Grossi, V.; Bakkas, S.; Rontani, J.-F. Visible light-dependent degradation of long-chain alkenes in killed cells of *Emiliania huxleyi* and *Nannochloropsis salina*. *Phytochemistry* **2001**, *56*, 677-684.
- 742
- 743 [86](#). Rontani, J.-F.; Marty, J.-C.; Miquel, J.-C.; Volkman, J.K. Free radical oxidation (autoxidation) of alkenones and other microalgal lipids in seawater. *Organic Geochemistry* **2006**, *37*, 354-368.
- 744
- 745 [87](#). Rontani, J.-F.; Volkman, J.K.; Prahl, F.G.; Wakeham, S.G. Biotic and abiotic degradation of alkenones and implications for paleoproxy applications: a review. *Organic Geochemistry* **2013**, *59*, 95-113.
- 746
- 747 [88](#). Britton, G. Structure and properties of carotenoids in relation to function. *The FASEB Journal* **1995**, *9*, 1551-1558.
- 748
- 749 [89](#). Boon, C.S.; McClements, D.J.; Weiss, J.; Decker, E.A. Factors influencing the chemical stability of carotenoids in foods. *Critical Reviews in Food Science and Nutrition* **2010**, *50*, 515-532.
- 750
- 751 [90](#). Tan, B.L.; Norhaizan, M.E. Carotenoids: how effective are they to prevent age-related diseases? *Molecules* **2019**, *24*, 1801.
- 752
- 753 [91](#). Fiedor, J.; Fiedor, L.; Haeßner, R.; Scheer, H. Cyclic Endoperoxides of β -Carotene, potential pro-oxidants, as products of chemical quenching of singlet oxygen. *Biochimica et Biophysica Acta – Bioenergetics* **2005**, *1709*, 1-4.
- 754
- 755 [92](#). Ramel, F.; Birtic, S.; Ginies, C.; Soubigou-Taconnat, L.; Triantaphylidès, C.; Havaux, M. Carotenoid oxidation products are stress signals that mediate gene responses to singlet oxygen in plants. *Proceedings of the National Academy of Sciences* **2012**, *109*, 5535-5540.
- 756
- 757 [93](#). Boon, C.S.; McClements, D.J.; Weiss, J.; Decker, E.A. Factors influencing the chemical stability of carotenoids in foods. *Critical reviews in food science and nutrition* **2010** *50*, 515-532.
- 758
- 759 [94](#). Rontani, J. F. *Lipid Oxidation Products: Useful Tools for Monitoring Photo-and Autoxidation in Phototrophs*. Cambridge Scholars Publishing, U.K., 2021; pp. 112-125.
- 760
- 761 [95](#). Kliman, M.; May, J.C.; McLean, J. A. Lipid analysis and lipidomics by structurally selective ion mobility-mass spectrometry. *Biochimica et Biophysica Acta (BBA)-Molecular and Cell Biology of Lipids* **2011**, *1811*, 935-945.

762
763